2021

High Frequency Concurrent Measurements in Watershed and Impaired Estuary Reveal Coupled DOC and Decoupled Nitrate Dynamics

Gopal K. Mulukutla
University of New Hampshire, Durham, gopal.mulukutla@unh.edu

Wilfred Wollheim
University of New Hampshire, Durham

Joseph Salisbury
University of New Hampshire, Durham

Richard O. Carey
Massachusetts Department of Environmental Protection

Thomas Gregory
University of New Hampshire

Authors
Gopal K. Mulukutla, Wilfred Wollheim, Joseph Salisbury, Richard O. Carey, Thomas Gregory, and William H. McDowell

High Frequency Concurrent Measurements in Watershed and Impaired Estuary Reveal Coupled DOC and Decoupled Nitrate Dynamics.

Gopal K. Mulukutla [1], **Wilfred M. Wollheim**[1,2], **Joseph E. Salisbury**[3], **Richard O. Carey**[4], **Thomas K. Gregory**[3] **and William H. McDowell**[2]

[1]Earth Systems Research Center, University of New Hampshire, Durham, New Hampshire, USA.

[2]Department of Natural Resources and the Environment, University of New Hampshire, Durham, New Hampshire, USA

[3]Ocean Processes Analysis Laboratory, University of New Hampshire, Durham, New Hampshire, USA

[4] Massachusetts Department of Environmental Protection, Worcester, Massachusetts, USA

Key Points:

- Simultaneous water quality measurements in watershed and N-impaired estuary show strong watershed control for estuarine DOC but complex coupling for nitrate.
- DOC exhibited near-conservative behavior in the estuary.
- For nitrate, watershed spatial distribution of sources and interaction with estuarine internal process to produce complex response.

Corresponding author: Gopal Mulukutla (gopal.mulukutla@unh.edu)

Abstract

Rapid changes in land use, pollution inputs, and climate are altering the quantity, timing and form of materials delivered from watersheds to estuaries. To better characterize these alterations simultaneous measurements of biogeochemical conditions in watersheds and estuaries over a range of times scales are needed. We examined the strength of watershed-estuarine biogeochemical coupling using data of *in situ* measurements of nitrate, terrestrial dissolved organic carbon (DOC) and chloride collected over a seven-month period in a nitrogen impaired estuary in the northeastern US. The watershed was observed exerting strong control over concentrations of terrestrially derived DOC in the estuary, attributable to relative homogeneity of watershed sources derived from forested land use combined with relatively conservative behavior in estuarine waters. Estuarine nitrate patterns were more complex, suggesting the influence of heterogeneous watershed distribution of non-point and point sources and high reactivity of nitrate in the estuary. Understanding estuarine biogeochemical patterns will be advanced through greater use of simultaneous sub-hourly measurements of inflows, salinity and water quality estuaries and their upstream watersheds.

1.0 Introduction

Estuaries are strongly influenced by inputs of freshwater, nutrients, and carbon from coastal watersheds. The degree of influence is determined by several factors that can vary over space and time, including magnitude and frequency of storms, estuarine residence time relative to watershed area, the degree of anthropogenic activity, and consequent changes in land use composition (Arndt et al., 2007; Pinckney et al., 2001; Salisbury et al., 2008; Swaney et al., 2008). Eutrophication of estuarine waters due to N enrichment is increasing, causing many problems such as loss of biodiversity, increased algal blooms, anoxic water, acceleration of species invasions, and shifts in dominant biogeochemical pathways (Barbier et al., 2011; McClelland & Valiela, 1998; Smyth et al., 2013; Wetz & Yoskowitz, 2013). Watershed inputs of DOC to coastal areas are also occurring, potentially impacting light regimes and foodwebs (Balch et al., 2016). As a result, the ability of estuaries to provide important ecosystem services is continuing to decline (Deegan et al., 2012; Grabowski & Peterson, 2007).

Human activities alter the amount and timing of nutrient and organic matter inputs delivered to estuaries (Bowen & Valiela, 2008). Both watershed drivers and estuarine responses are further influenced by factors such as climate change and associated changes in temperature, sea levels, wind patterns, and the hydrologic cycle(Bricker et al., 2008; Salisbury et al., 2009; Statham, 2012). Increases in anthropogenic N and changes to organic matter fluxes are occurring in the watershed due to expanding agriculture, urbanization, and associated land use change. Although much anthropogenic N is retained in watersheds (Boyer et al., 2002) increased loading leads to increased export through rivers and streams (Seitzinger & Kroeze, 1998). Estuaries modulate exports of DOC (and other forms of carbon) with high *in situ* production rates, and spatial and temporal heterogeneity(Bauer et al., 2013). This has resulted in studies that report near-conservative behavior of DOC in some estuaries(Mantoura & Woodward, 1983; Vallino et al., 2005), non-conservative behavior in some (McKenna, 2004), while laboratory studies show terrestrial DOC to be highly reactive due to "salting out" or microbial degradation(Battin et al., 2009; Moran et al., 1999; Schlesinger & Bernhardt, 2013). Furthermore, hydrologic conditions can strongly influence the mobilization, transport, and retention of nutrients and carbon within watersheds (Kaushal et al., 2014; Morse & Wollheim, 2014). Thus, with climate change, the controlling mechanisms of estuarine conditions will also likely change.

Watershed-estuary coupling can occur continuously during periods of baseflow or episodically during stormflow. An estuary responds to watershed and environmental drivers over multiple temporal scales (Cloern & Nichols, 1985) (a) short duration driven by daylight or tides, (b) storm event scale, driven by freshwater inflows lasting hours to weeks, (c) seasonal, due to changes in precipitation, temperature, and watershed function, and (d) annual, due to longer term climate oscillations and trends. Previous estuarine studies focused on seasonal or annual time scales that combined infrequent observations of biogeochemical characteristics (e.g., weekly or monthly) with finer temporal scale observations of inflows (Clair et al., 2013; Valiela & Bowen, 2002). However, a focus on broader time scales limits understanding of estuarine responses at finer time scales (Bergamaschi, Fleck, et al., 2012; Bergamaschi, Krabbenhoft, et al., 2012; Robins et al., 2018). For example, during storms, patterns in N concentration exported from watersheds may exhibit increase, decrease or remain chemostatic with flow depending watershed or time period(Godsey et al., 2009). Estuarine storm response may or may not reflect watershed patterns due to complicated circulation, stratification, or strong biological activity. Knowledge of these patterns often requires simultaneous sub-daily measurements in both watershed and estuary.

The emergence of *in situ* sensor technologies capable of continuous biogeochemical measurements provide opportunities to improve the understanding of watershed-estuary linkages (Bergamaschi, Krabbenhoft, et al., 2012). Sensors can perform autonomous high temporal frequency (sub-hourly) and long term (>3 months) measurements of key biogeochemical variables including nitrate, phosphate, and dissolved organic carbon (DOC) via an optical proxy (fluorescent dissolved organic matter, fDOM)(Downing et al., 2012), as well as classic water quality parameters in watersheds (Carey et al., 2014; Saraceno et al., 2009) and marine waters (O'Boyle et al., 2014). However, only a few studies have implemented concurrent watershed-estuary systems to study biogeochemical coupling and its implications for estuarine conditions (Gilbert et al., 2013).

The objective of this study was to examine seasonal and storm event dynamics of estuarine nitrate and DOC using simultaneous measurements of river and estuarine chemistry. We conducted this study in Great Bay, New Hampshire, USA, and in the watershed of its largest tributary, Lamprey River. This estuary system faces long-term land-use change and increasing climate variability. We hypothesized that: a) storm-event watershed nitrate and DOC fluxes will provide greater control on corresponding estuarine concentrations and that the estuary will show minimal coupling during baseflow, b) due to the spatial homogeneity of watershed sources, estuarine DOC will respond more to storm-event watershed DOC fluxes than estuarine nitrate to nitrate fluxes, and c) for both nitrate and DOC, monitoring in one sub-watershed will not be fully representative of variability observed in estuarine conditions.

2.0 Study Site and Methods

The Great Bay estuary is located in Northeastern USA (Figure 1). The estuary system consists of nine major sub-watersheds formed by seven major tributaries (Table 1). The watershed (2651 km^2) has a population of 400,000 people living in 55 urbanizing municipalities (Mills, 2009; P Trowbridge et al., 2014; Phil Trowbridge, 2007). The estuarine system is strongly tidal with relatively shallow morphology marked by limited vertical stratification (Short, 1992), a large volume relative to inputs, and long baseflow residence time (13-20 days, Text S1, supporting information). Great Bay is showing signs of eutrophication attributed mainly to nitrogen over-enrichment from both point (32%) and non-point sources (68%) (PREP, 2013). Increased N loads (42%) in recent years (Bresler, 2012; P. Trowbridge, 2010) have contributed to greater prevalence of phytoplankton and nuisance macroalgae, and leading the US-EPA to list it as N-impaired with regulations proposed such as expensive upgrades to waste water treatment plants (WWTP). Increased storm activity in the region (Douglas et al., 2011) has also increased inputs of terrestrial DOC and turbidity to coastal waters (Balch et al., 2016). Together, these changes have led to reduced water clarity and light penetration, possibly contributing to an observed drastic reduction in the spread of eelgrass, the estuary's cornerstone vegetation (Beem & Short, 2009). Focus of this study is Great Bay proper, the largest sub-estuary in the estuarine system, and the Lamprey River sub-watershed (Figure 1).

2.1 Measurements

Continuous, high frequency (every 30 minutes) measurements of nitrate, fDOM and conductance/salinity were made using *in situ* sensors deployed simultaneously in the estuary and its tributary, the Lamprey River (Figure 2). Sensors were deployed for one growing season (May - November 2011). River flow data were obtained from a co-located discharge gage operated by the US Geological Survey (#01073500 Lamprey River near Newmarket, NH). A linear regression between weekly grab measurements (DOC, NO_3, and, Cl) and corresponding sensor variable (fDOM, NO_3, specific conductance) was used to correct sensor measurements. Instantaneous watershed fluxes were estimated at a given instant of time, *f(t)* as:

$$f(t) = C(t) * Q(t) \qquad (2)$$

Where *C(t)* is the measured concentration of the constituent, and *Q(t)* is the flow across the river at time instant *t*.

2.3 Data Analysis Methods

<u>Data pre-processing</u>

Individual time series variables were first quality controlled by removing outliers and replacing them initially with an "NaN" (not a number). Missing data points were also identified using an "NaN". Segments of data with "NaNs" were then linearly interpolated to remove any missing data and make the time series temporally continuous allowing the application of time series techniques described below. Tidal influences on the time series of estuarine variables were removed using a low-pass filter (Johnson et al., 2006). According to this procedure, the Fourier transform of the signal was first computed. The amplitude of spectral frequencies higher than 1.375 cycles per day were zeroed to remove the dominant semi-diurnal component. The signal was then reconstructed through an inverse Fourier transform. The reconstructed signal developed by applying this technique contains only the weaker tidal frequencies along with any variability caused by diel biological processing.

<u>Time series methods</u>

We applied *frequency dependent coherence,* (C; 0<C<1) a time series analysis technique, to evaluate how estuarine concentrations (NO_3, fDOM and Cl) vary over time in conjunction with a related watershed variable (freshwater inflows; NO_3, DOC and Cl concentration and fluxes). Given two time series u(t) and v(t) *frequency dependent coherence* within a narrow band of frequency ($\Delta\omega$) with center at ω_o is given as (Menke & Menke, 2012)

$$C_{uv}{}^2(\omega_0\,,\Delta\omega) = \frac{|\tilde{u}^*(\omega_0)\tilde{v}(\omega_0)|^2}{|\tilde{u}(\omega_0)|^2|\tilde{v}(\omega_0)|^2} \qquad (2)$$

Where $\tilde{u}(\omega_0)$ and $\tilde{v}(\omega_0)$ are the Fourier transforms of u(t) and v(t), at frequency ω_0, respectively, and $\tilde{u}^*(\omega_0)$ is the Fourier transform of time reversed u(t), at frequency ω_0. The coherence profile is constructed by applying Eq. (2) over the entire frequency range of a signal. Coherence values reported here are denoted by subscripted variable $\overline{C}_{E-R}$, where overbar represents an average coherence over a given time period, and E and R represent (filtered) estuarine constituent concentration and watershed variable respectively.

<u>Storm Event Delineation</u>

We examined individual storm event patterns between estuarine concentrations and watershed nutrient fluxes (hysteresis) to determine intra-storm watershed-estuary coupling.

These patterns are analogous to the concentration-discharge relationships observed in watersheds (Carey et al., 2014; Evans & Davies, 1998). We analyzed 13 freshwater storm events for the influence of freshwater discharge, DOC, and NO_3 fluxes on estuarine concentration patterns. River flow data was obtained from a discharge gage operated by the US Geological Survey (USGS 01073500 Lamprey River near Newmarket, NH).

Each storm was partitioned by 3 points: the start of the storm (beginning of rising limb), peak flow (beginning of falling limb), and end of the storm (termination of falling limb). The beginning of a storm event was identified based on a minimum flow increase of 1.5 m^3/s (see Figure 3). The end of storm was determined by identifying the earliest point since the beginning of a storm that was within 0.5 m^3/s of observed baseflow. Some storm events constituted two or more high flow points; a consequence of a lull followed by more precipitation. For this study such events were identified as a single storm event with highest among the multiple high flows identified as peak storm flow. Also, the beginning of the increase in flow identified for the earliest peak and the end of the flow identified for the latest peak were selected as the beginning and end of the storm event respectively (Figure 3).

Storm characteristics examined include: overall estuarine concentration response (increase/decrease), rotational pattern (clockwise/anti-clockwise/multi-loop), and degree of coupling between watershed and estuary where degree of storm event-scale coupling is defined using a power-law function, $P=b\,F^{\alpha}$, where P is estuarine constituent concentration, F is watershed flux of a given constituent, b and α are fitted parameters(Basu et al., 2010; Godsey et al., 2009). We applied this to individual rising and falling limbs of storm-event watershed inputs. An α (estuarine responsiveness) that is positive indicates increased estuarine concentrations resulting from storm inputs. A zero or non-significant exponent indicates no coupling, while a negative exponent indicates declining concentrations resulting from storm inputs.

3 Results

3.1 Watershed and Estuarine Biogeochemical Patterns

Estuarine fDOM tracks well with watershed DOC fluxes (Figure 2a), with a pattern of high concentrations observed during high runoff in spring and autumn (~60 quinine sulfate equivalent parts per billion (QSE-ppb)) and lower concentrations during summer low flows (~30 QSE-ppb). Terrestrial DOC is the major portion of observed fDOM response (4.04 QSE-ppb recorded at salinity of 32 psu). Through the rest of this discussion fDOM will be used interchangeably with "terrestrial DOC". Each storm event peak in DOC flux is followed closely by a peak in fDOM. Watershed NO_3 fluxes and estuarine NO_3 concentrations (Figure 2b) also show high levels in late spring and fall (0.1-0.2 mg NL^{-1}), and lows in the summer (<0.05 mg NL^{-1}). But in contrast to fDOM, estuarine NO_3 concentrations show less pronounced response to storm-event flows (Figure 2b).

Partitioning response time scales provided by coherence analysis allows insights into watershed-estuary coupling. *Frequency dependent coherence* response of each estuarine constituent (Cl, fDOM, NO_3 concentrations) was examined by pairing initially with watershed discharge (Figure 4a) and then with respective watershed concentrations (Figure 4b) and flux (Figure 4c). Given that river discharge varies over several orders of magnitude while concentrations of most constituents are less variable (Godsey et al., 2009; Kirchner & Neal, 2013), we would expect that coherence between estuarine concentrations and watershed fluxes would be stronger than coherence between estuary and watershed concentrations

Over the study period using time scales greater than one day the average coherence of estuarine constituent concentrations was highest when related to watershed discharge (Table 3) with all three constituents exhibiting similar levels of coherence ($\overline{C}_{NO3-Q} = 0.21$, $\overline{C}_{fDOM-Q} = 0.22$, $\overline{C}_{Cl-Q} = 0.17$). Coherence was much lower when relating estuarine concentrations with watershed concentrations ($\overline{C}_{NO3-NO3} = 0.05$, $\overline{C}_{fDOM-DOC} = 0.09$, $\overline{C}_{Cl-Cl} = 0.11$)(Figure 4b). Coherence between estuarine DOC and Cl and corresponding watershed DOC and Cl fluxes were similar to those when using discharge, while coherence between estuarine NO_3 and watershed NO_3 fluxes was lower than when using discharge ($\overline{C}_{NO3-NO3flux} = 0.13$, $\overline{C}_{fDOM-DOCflux} = 0.21$, $\overline{C}_{Cl-Clflux} = 0.16$).

Over long time scales (>100 days) coherences were high between estuarine fDOM, NO_3, and Cl and corresponding watershed constituent fluxes (Figure 4c, $\overline{C}_{NO3-NO3flux} = 0.99$, $\overline{C}_{fDOM-DOCflux} = 0.95$, $\overline{C}_{Cl-Clflux} = 0.73$) indicating the predominant role of freshwater inputs over seasonal time scales . Likewise, coherences between concentrations and fluxes over short time scales (< 6 days) are very low ($\overline{C}_{NO3-NO3flux} = 0.07$, $\overline{C}_{fDOM-DOCflux} = 0.11$, $\overline{C}_{Cl-Clflux} = 0.07$) suggesting the watershed has minimal influence over estuarine variability over these time scales.

At intermediate time scales (6 - 30 days), a time span that encompasses storm flows (Table 1), the response of estuarine concentrations to watershed fluxes for all three constituents was observed to be intermediate in magnitude. Coherence between estuarine concentrations and watershed flux was much greater than when using watershed concentration across all time scales (Figure 4b) and were similar or lower than when using discharge (Figure 4a).

When using watershed fluxes, NO_3 coherence was lower than DOC or Cl across all time scales, and especially during intermediate scales (Figure 4c). For both Cl and DOC, there is a broad peak approached by around 7 days (Figure 4c) with declines occurring around 20 days. In contrast, NO_3 coherence also peaks around 7-9 days but the decline occurs much earlier and rapidly at around 15 days. Average coherence during this period is higher for DOC than for NO_3 ($\overline{C}_{fDOM-DOCflux} = 0.67$, $\overline{C}_{NO3-NO3flux} = 0.38$). The observed response at intermediate time scale is a collective indication of watershed inputs from all storm events.

These results suggest that over the course of the year flows drive variability in estuarine concentrations, while changes in watershed concentrations are secondary. Although coherence with discharge was similar or better when using watershed fluxes, we chose constituent fluxes as the basis for further study because in principle they should provide better coherence and because time scales where this is not true may be informative.

3.2 Storm Event Patterns

In our examination of storm-event patterns in estuarine concentration Vs. watershed fluxes, some hysteresis naturally occurs due to the spatial separation between watershed and estuarine monitoring locations. Consequently, the peak/minimum in the estuarine variable occurs after the peak/minimum in the watershed variable. We did not correct the data for such lags. However, where it could be characterized lags were found to not affect our results (section S2, supporting information).

The hysteresis response observed over the whole period of deployment (Figure 5) the estuarine response is a superposition of loops organized by season and estuary responding positively to increased watershed fluxes. In contrast, individual storm response is complex as shown in hysteresis plots in the supporting information(Figures S1-S13). Storms generally modify estuarine conditions from the pre-storm state for each constituent (Figure 2), but the strength of response varies with constituent, storm size and time of year. Initial conditions, just prior to a storm-event, for nitrate and DOC show a strong positive correlation with watershed fluxes, while Cl shows a strong negative correlation (Figure 6)(DOC: R^2 =0.72; NO_3: R^2=0.87; Cl: R^2=0.79, all $p<0.05$).

Storms generally tend to increase fDOM and NO_3 and reduce Cl (salinity), in the estuary. fDOM and Cl hysteresis patterns (Table 2) show consistent, anti-clockwise and clockwise response, respectively, with only two low intensity storms showing changes in rotational pattern. NO_3 hysteresis patterns are more complex, with 6 of 13 storms recording a multi-loop pattern (Figure 5c and Figures S1-S13, supporting information). Responsiveness (α) along the rising limb did not show a significant relationship with storm runoff (R^2 =0.05; p >0.05), precipitation amount (R^2 = 0.12; p >0.05) or rising limb duration (R^2 = 0.07; p >0.05) (Figure 7a-c). However, all but two storms show a net concentrating response on the rising limb ($\overline{\alpha}^{+}_{NO3-RL}$ = 0.254, p<0.05) and a weak response on the falling limb. Relatively large storms during late summer elicited only a small estuarine NO_3 response, despite the occurrence of two relatively intense events (e.g. storms 6 and 9 relative to storm 1 and 3, Table 2). Small storms of relatively short duration (6 - 7 days) elicited in multi-loop patterns. Several storms (storms 2, 6, 7 and 13) showed a small initial pulse in estuarine NO_3 concentration at the beginning of the rising limb.

For fDOM the responsiveness for rising limb (α_{DOC-RL}) showed an increase with duration (R^2 = 0.61; p <0. 05), total storm event discharge (R^2 =0.50; p <0.05), and total precipitation amounts (R^2 = 0.37; p <0.05) (Figure 8a – c) with higher responsiveness for larger storms. Corresponding results for falling limb of the storm-event were weaker. The hysteresis patterns of Cl are nearly inverse those of fDOM, (Figure 5). Five storm events (storm 2, 6, 10, 12 and 13) showed slightly increasing salinity along the rising limb ($\alpha_{Cl-RL} > 0$) (Figure S2, S6, S10,S12 and S13). Estuarine fDOM for the same storms showed slight dilution with increasing DOC fluxes ($\alpha_{DOC-RL} < 0$). The responsiveness patterns for Cl is weaker (Figure 9), but clearly the opposite of fDOM response.

4 Discussion

4.1 Watershed Control of Estuarine DOC

Past studies in watersheds have shown that constituent concentration vs. discharge hysteresis occurs due to preferential delivery (source or transport limitation) of water and nutrients(Camporese et al., 2014; Dusek & Vogel, 2016; Lloyd et al., 2016; Phillips, 2003). Complicated multi-loop patterns have also been attributed to complex catchment response (Williams, 1989). Strong fDOM responsiveness observed with duration of rising limb of storm hydrograph, increased runoff, and precipitation, and combined with a weaker response on the falling limb suggests that watershed-estuary connectivity is similar to hydrologic connectivity observed between watershed, and a headwater stream or river (Kaller et al., 2015; Nippgen et al., 2015). Counter to general patterns, some smaller storms resulted in increased Cl and dilution of fDOM. Elevated influx of ocean water that counter increases in freshwater of terrestrial DOC inputs can cause such a dynamic (Huang et al., 2014). Also, the changing quality of DOC exported from watersheds can vary over storm events causing changes in the fDOM response (Larsen et al., 2015). However these factors were not of sufficient magnitude to confound the overall coherence response. Hysteresis analysis demonstrated the strong influence of watershed over estuarine DOC conditions over storm-event time scales (Figure 5, Table 2).

DOC in both freshwaters and estuaries is derived mainly from forests and wetland (Buffam et al., 2001; Creed et al., 2003). The Lamprey River sub-watershed (21% of total watershed area) consists of 82% forest and wetlands, compared to 74% for the whole watershed (Table 1). Although DOC concentrations in northeastern watersheds increase with discharge, their variability is smaller than the orders of magnitude variation observed in discharge (Raymond & Saiers, 2010). Indeed, the coherence between estuarine fDOM and discharge was just as strong as when using DOC fluxes. Which leads us to conclude terrestrial DOC variability captured by monitoring one sub-watershed was sufficient to explain the overall dynamics of DOC in the estuary, including inputs from unmonitored areas. As a result, watershed DOC exports may be sufficiently well predicted by commonly used, less intensive methods combining continuous flow and infrequent grab measurements.

Factors that increase runoff from watersheds will also increase DOC exported to coastal zones. This suggests that greater watershed-estuary coupling will occur in the future where more frequent extreme events are predicted to occur (Hayhoe et al., 2007). More recently, reports indicate that terrestrial DOC is already increasing in coastal oceans in response to changing storm patterns (Balch et al., 2016). Impacts of higher fDOM in estuaries and coastal ocean include increased light attenuation and altered food webs (Traving et al., 2017). In Great Bay, eel grass has been in decline in recent years (Beem & Short, 2009). Among the hypotheses attributed to this decline is a greater frequency of light limitation due to higher fDOM, similar to estuaries elsewhere (Ganju et al., 2014). Which suggests the changing role of watershed DOC fluxes, along with other interacting factors (e.g. suspended sediment flux and resulting turbidity) should be considered in coastal management.

4.2.Conservative Behavior of Terrestrial DOC in the Estuary

DOC and Cl coherence response is very similar in the time scale of 1-180 days Hysteresis data provides more evidence of this similarity. Estuarine fDOM response is similar albeit nearly inverse storm event chloride (Figures 5). The inverse pattern for Cl is expected when behavior is assumed to be conservative because chloride in the estuary should decline during storms (since more freshwater with less Cl than in the estuary), while fDOM in the estuary should increase (since more freshwater with more DOC than in the estuary). The fact that chloride is conservative, and the symmetrical and inverse behavior of fDOM over the 1-180 day time scale strongly suggests that fDOM behaves in a (near-) conservative way. This behavior may be explained by the presence of simultaneous sources and sinks leading to minimal turnover within the estuary (Mantoura & Woodward, 1983) or by the removal of specific components of the DOC pool (Raymond & Spencer, 2014).

Conservative behavior of terrestrial DOC has been observed in a freshwater coastal river network of New England (Wollheim et al., 2015) as well as in larger North American river networks, unless there are long residence-time features in surface waters, such as large lakes or reservoirs (Hanley et al., 2013). Because of relatively little transformation of terrestrial DOC in the estuary, combined with the importance of transport limitation for riverine carbon transport (Bauer et al., 2013) much of this DOC may eventually make its way to the coastal ocean, as observed in the Gulf of Maine where its fate and consequence remain poorly understood (Balch et al., 2016).

4.3 Complex Behavior of Estuarine NO_3

In the Lamprey R. watershed, suburban and agricultural land-cover, a major non-point source of nitrate (Wollheim et al., 2005) is 16% within this sub-watershed, and at 22 % in the whole watershed. Further, anthropogenic land uses are concentrated in several of the sub-watersheds (Table 1 and Figure 1) creating heterogeneity of inputs relative to the hydrodynamic circulation within the estuary. As a result, non-point N sources dominate annual loads, of which a substantial portion is exported during storm events, whereas baseflow is dominated by point N sources (PREP, 2013). Over seasonal time scales, nitrate's coherence response is similar to that of DOC and Cl. This may due to watershed (baseflow) influence on estuarine conditions and the predominance of point-sources over these time scales. This could also be due to the simple coincidence of the periods of high and low biological activity that leads to increased sources and reduced uptake occurring simultaneously in terrestrial, freshwater, and estuarine ecosystems. Monitoring multiple growing seasons will allow more insight into these patterns.

If estuarine nitrate were to behave like in river systems, point-source dominant baseflow patterns would lead to dilution during storm events (Colombo et al., 2004; Jiang et al., 2014). If non-point inputs dominate, then NO_3 concentrations would increase (Feinson et al., 2016). NO_3 concentrations generally increase during storms compared to pre-storm conditions, unlike Cl which exhibits dilution. This is an important pattern as it suggests that watershed non-point sources override any dilution effect of point-source (WWTP) and NO_3 uptake in watershed and estuary. Further evidence to this effect can be observed in the small initial pulse of nitrate observed during four events that has also been reported in the watershed (Carey et al., 2014), possibly a small signature of non-point source inputs from developed areas downstream of the watershed monitoring station. Thus, non-point sources are a significant control of estuarine nitrate, just as it is for estuarine fDOM with watershed DOC.

Direct point-source inputs to the estuary likely do not vary considerably during storm events because of the absence of major combined sewer overflows in this watershed (NHDES, 2009). However, hydrodynamics may change during freshwater pulses (Zorndt et al., 2012) so the relative importance of point and non-point sources from different parts of the watershed may confound the estuarine signal. This also is apparent in the coherence response, where storm-event time scale coherence between watershed inputs and estuarine nitrate is greatly reduced, when compared with fDOM and Cl. This rapid dissipation of (the monitored) watershed NO_3 compared to terrestrial DOC signal in estuary, has been observed elsewhere (Mooney & McClelland, 2012). Unraveling causes behind this divergence in NO_3 (compared to DOC and Cl) is centrally important for management, as it would suggest a need to focus on reducing point or non-point sources, or alternatively, develop a better understanding the internal fate of estuarine NO_3.

Estuaries are thought to be important net transformers of nitrate along the continuum from terrestrial uplands to the open ocean (Galloway et al., 2003; S. Seitzinger et al., 2006). Net NO_3 removal during individual storm events could occur because of assimilation by macrophytes or algae, or via denitrification (Giblin et al., 2010; Kalnejais et al., 2007). The minimal response of NO_3 observed during intense late-summer storm events may be a result of internal estuarine processes resulting from warmer water (Hou et al., 2012; Ogilvie et al., 1997) (Figure 5c). The effectiveness of removal of watershed inputs will vary depending on distance traveled from location of watershed input and estuarine measurement location. In addition, catchment characteristics that contribute to the quantity and timing of storm flows exported from watersheds may also a play a role in the estuarine response. Geomorphology and basin geometry form a control on the shape and peak timing of storm hydrographs (Sólyom, 2004). Whereas, storm-event constituent concentrations are influenced by the spatial distribution of source material(Walling & Webb, 1980), leading to the formation of hotspots of reactivity, that play an important role in processing of nitrogen in river networks (Mineau et al., 2015). It is likely that similar modifications also occur in estuaries. These observations, taken together with the coherence response suggest that nitrate is spatially complex and its variability not well-predicted by the monitored watershed inputs, in contrast to terrestrial DOC discussed previously.

5.0 Conclusions

The use of simultaneous watershed-estuary measurements is a potentially powerful way to enhance understanding of estuarine conditions. It was exemplified here using continuous time series data and application of unique analysis techniques to examine temporal signatures of variability in estuarine nitrate and DOC and in the context of their watershed delivery mechanisms. Watershed control of nitrate and DOC was found to be strong in the baseflow-dominant seasonal and longer time scales. But strong differences were revealed in intermediate, storm-event time scales, with DOC exhibiting stronger connectivity with the watershed, and nitrate showing complex patterns.

While, the DOC behavior was attributable to the relatively homogenous distribution of sources, leading to near conservative behavior over the 6-180-day time scale, a combination of factors led to the complex behavior of nitrate. Among them, sporadic distribution of sources, point-source dominant baseflow, non-point source dominant rapid depletion during storm events, and the spatially-variable highly reactive NO_3 interacting with estuarine assimilatory and dissimilatory processes. Due to this homogenous nature of DOC sources, spatially limited but representative monitoring of DOC would be sufficient to capture its dynamics in the estuary. However, for nitrate, automated, appropriately scaled, sensor-based monitoring would be essential to meet the spatial resolution necessary in this watershed, and other impaired watersheds, where human activities have resulted in the formation of a heterogenous patches of sources and sinks. Such monitoring programs would need to be integrated with estuarine hydrodynamic models (Ganju et al., 2016) with input of high resolution data of multiple elements (here DOC, Cl, and NO_3) to understand the spatially and temporally complex patterns (e.g. Testa et al., 2014). With human and climate driven alterations of coastal ecosystems continuing to occur automated, simultaneous watershed-estuary biogeochemical measurements are essential, not only to develop targeted and effective, nutrient-management activities but also to understand and predict climate-driven changes to exports of nutrients and carbon to the coastal waters.

6.0 Acknowledgements

This research was funded in part by NSF (EPS 1101245), NH Sea Grant (NOAA NA10OAR4170082), NH Agricultural Experiment Station and UNH ESRC's Iola Hubbard Endowment for Climate Change. This is AES Scientific Contribution Number 2675 supported by the USDA NIFA Hatch Project 0225006. Data underlying this work is provided with the supporting information. The underlying raw data and associated metadata is provided in the supporting information. Code related to the use of frequency dependent coherence is available upon request.

References

Arndt, S., Vanderborght, J. P., & Regnier, P. (2007). Diatom growth response to physical forcing in a macrotidal estuary: Coupling hydrodynamics, sediment transport, and biogeochemistry. *Journal of Geophysical Research: Oceans*, *112*(5). https://doi.org/10.1029/2006JC003581

Balch, W., Huntington, T., Aiken, G., Drapeau, D., Bowler, B., Lubelczyk, L., & Butler, K. (2016). Toward a quantitative and empirical dissolved organic carbon budget for the Gulf of Maine, a semienclosed shelf sea. *Global Biogeochemical Cycles*, *30*(2), 268–292. https://doi.org/10.1002/2015GB005332

Barbier, E. B., Hacker, S. D., Kennedy, C., Koch, E. W., Stier, a. C., & Silliman, B. R. (2011). The value of estuarine and coastal ecosystem services. *Ecological Monographs*, *81*(2), 169–193. https://doi.org/10.1890/10-1510.1

Basu, N. B., Destouni, G., Jawitz, J. W., Thompson, S. E., Loukinova, N. V., Darracq, A., et al. (2010). Nutrient loads exported from managed catchments reveal emergent biogeochemical stationarity. *Geophysical Research Letters*, *37*(23), 1–5. https://doi.org/10.1029/2010GL045168

Battin, T. J., Kaplan, L. a., Findlay, S., Hopkinson, C. S., Marti, E., Packman, A. I., et al. (2009). Biophysical controls on organic carbon fluxes in fluvial networks. *Nature Geoscience*, *2*(8), 595–595. https://doi.org/10.1038/ngeo602

Bauer, J. E., Cai, W.-J., Raymond, P. A., Bianchi, T. S., Hopkinson, C. S., & Regnier, P. A. G. (2013). The changing carbon cycle of the coastal ocean. *Nature*, *504*(7478), 61–70. https://doi.org/10.1038/nature12857

Beem, N. T., & Short, F. T. (2009). Subtidal eelgrass declines in the Great Bay Estuary, New Hampshire and Maine, USA. *Estuaries and Coasts*, *32*(1), 202–205. https://doi.org/10.1007/s12237-008-9110-3

Bergamaschi, B. A., Fleck, J. A., Downing, B. D., Boss, E., Pellerin, B. A., Ganju, N. K., et al. (2012). Mercury Dynamics in a San Francisco Estuary Tidal Wetland: Assessing Dynamics Using In Situ Measurements. *Estuaries and Coasts*, *35*(4), 1036–1048. https://doi.org/10.1007/s12237-012-9501-3

Bergamaschi, B. A., Krabbenhoft, D. P., Aiken, G. R., Patino, E., Rumbold, D. G., & Orem, W. H. (2012). Tidally driven export of dissolved organic carbon, total mercury, and methylmercury from a mangrove-dominated estuary. *Environmental Science and Technology*, *46*(3), 1371–1378. https://doi.org/10.1021/es2029137

Bowen, J. L., & Valiela, I. (2008). N to Assess Coupling between Watersheds and Estuaries in Temperate and Tropical Regions. *Journal of Coastal Research*, *243*(243), 804–813. https://doi.org/10.2112/05-0545.1

Boyer, E. W., Goodale, C. L., Jaworski, N. A., & Howarth, R. W. (2002). Anthropogenic nitrogen sources and relationships to riverine nitrogen export in the northeastern U.S.A. *Biogeochemistry*, *57–58*, 137–169. https://doi.org/10.1023/A:1015709302073

Bresler, S. E. (2012). Policy recommendations for reducing reactive nitrogen from wastewater treatment in the Great Bay Estuary, NH. *Environmental Science and Policy*, *19–20*, 69–77. https://doi.org/10.1016/j.envsci.2012.02.006

Bricker, S. B., Longstaff, B., Dennison, W., Jones, A., Boicourt, K., Wicks, C., & Woerner, J. (2008). Effects of nutrient enrichment in the nation's estuaries: A decade of change. *Harmful Algae*, *8*(1), 21–32. https://doi.org/10.1016/j.hal.2008.08.028

Buffam, I., Galloway, J. N., & Blum, L. K. (2001). A storm ow/base ow comparison of dissolved organic matter concentrations and bioavailability in an Appalachian stream. *Biogeochemistry*, 269–306.

Camporese, M., Penna, D., Borga, M., & Paniconi, C. (2014). A field and modeling study of nonlinear storage-discharge dynamics for an Alpine headwater catchment. *Water Resources Research*, *50*(2), 806–822. https://doi.org/10.1002/2013WR013604

Carey, R. O. R. O., Wollheim, W. M. W. M., Mulukutla, G. K. G. K., & Mineau, M. M. M. M. (2014). Characterizing storm-event nitrate fluxes in a fifth order suburbanizing watershed using in situ sensors. *Environmental Science and Technology*, *48*(14), 7756–7765. https://doi.org/10.1021/es500252j

Clair, T. A., Dennis, I. F., & Bélanger, S. (2013). Riverine nitrogen and carbon exports from the Canadian landmass to estuaries. *Biogeochemistry*, *115*(1–3), 195–211. https://doi.org/10.1007/s10533-013-9828-2

Cloern, J. E., & Nichols, F. H. (1985). Time scales and mechanisms of estuarine variability, a synthesis fromstudies of san francisco bay. *Hydrobiologia.*, *12*, 229–237.

Colombo, M. J., Grady, S. J., & Trench, E. (2004). *Nutrient Enrichment , Phytoplankton Algal Growth , and Estimated Rates of Instream Metabolic Processes in the Quinebaug River Basin , Connecticut , 2000 – 2001 Scientific Investigations Report 2004-5227* (pp. 2000–2001).

Creed, I. F., Sanford, S. E., Beall, F. D., Molot, L. A., & Dillon, P. J. (2003). Cryptic wetlands: Integrating hidden wetlands in regression models of the export of dissolved organic carbon from forested landscapes. *Hydrological Processes*, *17*(18), 3629–3648. https://doi.org/10.1002/hyp.1357

Deegan, L. a., Johnson, D. S., Warren, R. S., Peterson, B. J., Fleeger, J. W., Fagherazzi, S., & Wollheim, W. M. (2012). Coastal eutrophication as a driver of salt marsh loss. *Nature*, *490*(7420), 388–392. https://doi.org/10.1038/nature11533

Douglas, E. M., Asce, M., & Fairbank, C. A. (2011). Is Precipitation in Northern New England Becoming More Extreme ? Statistical Analysis of Extreme Rainfall in Massachusetts , New Hampshire , and Maine and Updated Estimates of the 100-Year Storm. *Most*, *16*(3), 203–218. https://doi.org/10.1061/(ASCE)HE.1943-5584.0000303.

Downing, B. D., Pellerin, B. a., Bergamaschi, B. a., Saraceno, J. F., & Kraus, T. E. C. (2012). Seeing the light: The effects of particles, dissolved materials, and temperature on in situ measurements of DOM fluorescence in rivers and streams. *Limnology and Oceanography: Methods*, *10*, 767–775. https://doi.org/10.4319/lom.2012.10.767

Dusek, J., & Vogel, T. (2016). Hillslope-storage and rainfall-amount thresholds as controls of preferential stormflow. *Journal of Hydrology*, *534*, 590–605. https://doi.org/10.1016/j.jhydrol.2016.01.047

Evans, C., & Davies, T. D. (1998). Causes of concentration/discharge hysteresis and its potential as a tool for analysis of episode hydrochemistry. *Water Resources Research*, *34*(1), 129. https://doi.org/10.1029/97WR01881

Feinson, L. S., Gibs, J., Imbrigiotta, T. E., & Garrett, J. D. (2016). Effects of Land Use and Sample Location on Nitrate-Stream Flow Hysteresis Descriptors during Storm Events. *Journal of the American Water Resources Association*, *52*(6), 1493–1508. https://doi.org/10.1111/1752-1688.12477

Galloway, J. N., Aber, J. D., Erisman, J. W., Seitzinger, S. P., Howarth, R. W., Cowling, E. B., & Cosby, B. J. (2003). The Nitrogen Cascade. *American Institute of Biological Sciences*, *53*(4), 341. https://doi.org/10.1641/0006-3568(2003)053[0341:TNC]2.0.CO;2

Ganju, N. K., Miselis, J. L., & Aretxabaleta, A. L. (2014). Physical and biogeochemical controls on light attenuation in a eutrophic, back-barrier estuary. *Biogeosciences*, *11*(24), 7193–7205. https://doi.org/10.5194/bg-11-7193-2014

Ganju, Neil K., Brush, M. J., Rashleigh, B., Aretxabaleta, A. L., del Barrio, P., Grear, J. S., et al. (2016). Progress and Challenges in Coupled Hydrodynamic-Ecological Estuarine Modeling. *Estuaries and Coasts*, *39*(2), 311–332. https://doi.org/10.1007/s12237-015-0011-y

Giblin, A. E., Weston, N. B., Banta, G. T., Tucker, J., & Hopkinson, C. S. (2010). The Effects of Salinity on Nitrogen Losses from an Oligohaline Estuarine Sediment. *Estuaries and Coasts*, *33*(5), 1054–1068. https://doi.org/10.1007/s12237-010-9280-7

Gilbert, M., Needoba, J., Koch, C., Barnard, A., & Baptista, A. (2013). Nutrient Loading and Transformations in the Columbia River Estuary Determined by High-Resolution In Situ Sensors. *Estuaries and Coasts*, *36*(4), 708–727. https://doi.org/10.1007/s12237-013-9597-0

Godsey, S. E., Kirchner, J. W., & Clow, D. W. (2009). Concentration-discharge relationships reflect chemostatic characteristics of US catchments. *Hydrological Processes*, *23*(13), 1844–1864. https://doi.org/10.1002/hyp.7315

Grabowski, J., & Peterson, C. (2007). Restoring Oyster Reefs to Recover Ecoystem Services. *Ecosystem Engineers: From Plants to Protists*, 405.

Hanley, K. W., Wollheim, W. M., Salisbury, J., Huntington, T., & Aiken, G. (2013). Controls on dissolved organic carbon quantity and chemical character in temperate rivers of North America. *Global Biogeochemical Cycles*, *27*(2), 492–504. https://doi.org/10.1002/gbc.20044

Hayhoe, K., Wake, C. P., Huntington, T. G., Luo, L., Schwartz, M. D., Sheffield, J., et al. (2007). Past and future changes in climate and hydrological indicators in the US Northeast. *Climate Dynamics*, *28*(4), 381–407. https://doi.org/10.1007/s00382-006-0187-8

Hou, L., Liu, M., Carini, S. A., & Gardner, W. S. (2012). Transformation and fate of nitrate near the sediment-water interface of Copano Bay. *Continental Shelf Research*, *35*, 86–94. https://doi.org/10.1016/j.csr.2012.01.004

Huang, W., Hagen, S., & Bacopoulos, P. (2014). Hydrodynamic Modeling of Hurricane Dennis Impact on Estuarine Salinity Variation in Apalachicola Bay. *Journal of Coastal Research*, 389–398. https://doi.org/10.2112/JCOASTRES-D-13-00022.1

Jiang, Y., Frankenberger, J. R., Bowling, L. C., & Sun, Z. (2014). Quantification of uncertainty in estimated nitrate-N loads in agricultural watersheds. *Journal of Hydrology*, *519*(PA), 106–116. https://doi.org/10.1016/j.jhydrol.2014.06.027

Johnson, K. S., Coletti, L. J., & Chavez, F. P. (2006). Diel nitrate cycles observed with in situ sensors predict monthly and annual new production. *Deep-Sea Research Part I: Oceanographic Research Papers*, *53*(3), 561–573. https://doi.org/10.1016/j.dsr.2005.12.004

Kaller, M. D., Keim, R. F., Edwards, B. L., Raynie Harlan, A., Pasco, T. E., Kelso, W. E., & Allen Rutherford, D. (2015). Aquatic vegetation mediates the relationship between hydrologic connectivity and water quality in a managed floodplain. *Hydrobiologia*, *760*(1), 29–41. https://doi.org/10.1007/s10750-015-2300-7

Kalnejais, L. H., Martin, W. R., Signell, R. P., & and Michael H. Bothner. (2007). Role of Sediment Resuspension in the Remobilization of Particulate-Phase Metals from Coastal Sediments. *Environmental Science & Technology*, *41*(7), 2282–2288. https://doi.org/10.1021/es061770z

Kaushal, S. S., McDowell, W. H., & Wollheim, W. M. (2014). Tracking evolution of urban biogeochemical cycles: past, present, and future. *Biogeochemistry*, *121*(1), 1–21. https://doi.org/10.1007/s10533-014-0014-y

Kirchner, J. W., & Neal, C. (2013). Universal fractal scaling in stream chemistry and its implications for solute transport and water quality trend detection. *Proceedings of the National Academy of Sciences of the United States of America*, *110*(30), 12213–8. https://doi.org/10.1073/pnas.1304328110

Larsen, L., Harvey, J., Skalak, K., & Goodman, M. (2015). Fluorescence-based source tracking of organic sediment in restored and unrestored urban streams. *Limnology and Oceanography*, *60*(4), 1439–1461. https://doi.org/10.1002/lno.10108

Lloyd, C. E. M., Freer, J. E., Johnes, P. J., & Collins, A. L. (2016). Using hysteresis analysis of high-resolution water quality monitoring data, including uncertainty, to infer controls on nutrient and sediment transfer in catchments. *Science of the Total Environment*, *543*, 388–404. https://doi.org/10.1016/j.scitotenv.2015.11.028

Mantoura, R. F. C., & Woodward, E. M. S. (1983). Conservative behaviour of riverine dissolved organic carbon in the Severn Estuary: chemical and geochemical implications. *Geochimica et Cosmochimica Acta*, *47*(7), 1293–1309. https://doi.org/10.1016/0016-7037(83)90069-8

McClelland, J. W., & Valiela, I. (1998). Linking nitrogen in estuarine producers to land-derived sources. *Limnology and Oceanography*, *43*(4), 577–585. https://doi.org/10.4319/lo.1998.43.4.0577

McKenna, J. (2004). DOC dynamics in a small temperate estuary: simultaneous addition and removal processes and implications on observed nonconservative behavior. *Estuaries*, *27*(4), 604–616. https://doi.org/10.1007/BF02907648

Menke, W., & Menke, J. (2012). 9 - Detecting correlations among data. In W. Menke & J. Menke (Eds.), *Environmental Data Analysis with MatLab* (pp. 167–201). Boston: Elsevier. http://dx.doi.org/10.1016/B978-0-12-391886-4.00009-X

Mills, K. (2009). *Ecological Trends in the Great Bay Estuary* (p. 46). Durham,NH: Great Bay National Estuarine Research Reserve. Retrieved from http://greatbay.org/documents/20th-gbnerr-report.pdf

Mineau, M. M., Wollheim, W. M., & Stewart, R. J. (2015). An index to characterize the spatial distribution of land use within watersheds and implications for river network nutrient removal and export. *Geophysical Research Letters*, *42*(16), 6688–6695. https://doi.org/10.1002/2015GL064965

Mooney, R. F., & McClelland, J. W. (2012). Watershed Export Events and Ecosystem Responses in the Mission-Aransas National Estuarine Research Reserve, South Texas. *Estuaries and Coasts*, 1–18. https://doi.org/10.1007/s12237-012-9537-4

Moran, M. A., Sheldon, W. M., & Sheldon, J. E. (1999). Biodegradation of Riverine Dissolved Organic Carbon in Five Estuaries of the Southeastern United States. *Estuaries*, *22*(1), 55. https://doi.org/10.2307/1352927

Morse, N. B., & Wollheim, W. M. (2014). Climate variability masks the impacts of land use change on nutrient export in a suburbanizing watershed. *Biogeochemistry*, *121*(1), 45–59. https://doi.org/10.1007/s10533-014-9998-6

NHDES. (2009). *Combined sewer overflows in New Hampshire. An NH Department of Environmental Services Factsheet*. *[Online]* (pp. 1–6). Concord, NH: NH Department of Environmental Services. https://doi.org/10.1016/S0273-1223(98)00802-6

Nippgen, F., McGlynn, B. L., & Emanuel, R. E. (2015). The spatial and temporal evolution of contributing areas. *Water Resources Research*, *51*(6), 4550–4573. https://doi.org/10.1002/2014WR016719

O'Boyle, S., Trickett, P., Partington, A., & Murray, C. (2014). Field testing of an optical in situ nitrate sensor in three Irish estuaries. *Biology and Environment*, *114*(1), 3318. https://doi.org/10.3318/BIOE.2014.02

Ogilvie, B., Nedwell, D. B., Harrison, R. M., Robinson, A., & Sage, A. (1997). High nitrate, muddy estuaries as nitrogen sinks: The nitrogen budget of the River Colne estuary (United Kingdom). *Marine Ecology Progress Series*, *150*(1–3), 217–228. https://doi.org/10.3354/meps150217

Phillips, J. D. (2003). Sources of nonlinearity and complexity in geomorphic systems. *Progress in Physical Geography*, *27*(1), 1–23. https://doi.org/10.1191/0309133303pp340ra

Pinckney, J. L., Paerl, H. W., Tester, P., & Richardson, T. L. (2001). The role of nutrient loading and eutrophication in estuarine ecology. *Environmental Health Perspectives*, *109*(SUPPL. 5), 699–706. https://doi.org/10.1289/ehp.01109s5699

PREP. (2013). State of Our Estuaries 2013, 48. https://doi.org/10.2217/pmt.13.66

Raymond, P. A., & Saiers, J. E. (2010). Event controlled DOC export from forested watersheds. *Biogeochemistry*, *100*(1), 197–209. https://doi.org/10.1007/s10533-010-9416-7

Raymond, P. A., & Spencer, R. G. M. (2014). Riverine DOM. In *Biogeochemistry of Marine Dissolved Organic Matter: Second Edition* (pp. 509–533). https://doi.org/10.1016/B978-0-12-405940-5.00011-X

Robins, P. E., Lewis, M. J., Freer, J., Cooper, D. M., Skinner, C. J., & Coulthard, T. J. (2018). Improving estuary models by reducing uncertainties associated with river flows. *Estuarine, Coastal and Shelf Science*, *207*, 63–73. https://doi.org/10.1016/j.ecss.2018.02.015

Salisbury, J., Vandemark, D., Hunt, C., Campbell, J., Jonsson, B., Mahadevan, A., et al. (2009). Episodic riverine influence on surface DIC in the coastal Gulf of Maine. *Estuarine, Coastal and Shelf Science*, *82*(1), 108–118. https://doi.org/10.1016/j.ecss.2008.12.021

Salisbury, J. E., Vandemark, D., Hunt, C. W., Campbell, J. W., McGillis, W. R., & McDowell, W. H. (2008). Seasonal observations of surface waters in two Gulf of Maine estuary-plume systems: Relationships between watershed attributes, optical measurements and surface pCO2. *Estuarine, Coastal and Shelf Science*, *77*(2), 245–252. https://doi.org/10.1016/j.ecss.2007.09.033

Saraceno, J. F., Pellerin, B. A., Downing, B. D., Boss, E., Bachand, P. A. M., & Bergamaschi, B. A. (2009). High-frequency in situ optical measurements during a storm event: Assessing relationships between dissolved organic matter, sediment concentrations, and hydrologic processes. *Journal of Geophysical Research: Biogeosciences*, *114*(4), 1–11. https://doi.org/10.1029/2009JG000989

Schlesinger, W. H., & Bernhardt, E. S. (2013). Chapter 6 - The Biosphere: Biogeochemical Cycling on Land. In W. H. Schlesinger & E. S. Bernhardt (Eds.), *Biogeochemistry (Third Edition)* (Third Edit, pp. 173–231). Boston: Academic Press. https://doi.org/10.1016/B978-0-12-385874-0.00006-6

Seitzinger, S., Harrison, J., Bohlke, J., Bouwman, A., Lowrance, R., Peterson, B., et al. (2006). Denitrification across landscaes and waterscapes: a synthesis. *Ecological Applications*, *16*(6), 2064–2090. https://doi.org/10.1890/1051-0761(2006)016[2064:DALAWA]2.0.CO;2

Seitzinger, S. P., & Kroeze, C. (1998). Global distribution of nitrous oxide production and n inputs in freshwater and coastal marine ecosystems. *Global Biogeochemical Cycles*, *12*(1), 93–113. https://doi.org/10.1029/97GB03657

Short, F. T. (1992). *The Ecology of the Great Bay Estuary, New Hampshire and Maine: an Estuarine Profile and Bibliography*.

Smyth, A. R., Thompson, S. P., Siporin, K. N., Gardner, W. S., McCarthy, M. J., & Piehler, M. F. (2013). Assessing Nitrogen Dynamics Throughout the Estuarine Landscape. *Estuaries and Coasts*, *36*(1), 44–55. https://doi.org/10.1007/s12237-012-9554-3

Sólyom, P. B. (2004). Effect of limited storm duration on landscape evolution, drainage basin geometry, and hydrograph shapes. *Journal of Geophysical Research*, *109*(F3), F03012. https://doi.org/10.1029/2003JF000032

Statham, P. J. (2012). Nutrients in estuaries - An overview and the potential impacts of climate change. *Science of the Total Environment*, *434*, 213–227. https://doi.org/10.1016/j.scitotenv.2011.09.088

Swaney, D. P., Scavia, D., Howarth, R. W., & Marino, R. M. (2008). Estuarine classification and response to nitrogen loading: Insights from simple ecological models. *Estuarine, Coastal and Shelf Science*, *77*(2), 253–263. https://doi.org/10.1016/j.ecss.2007.09.013

Testa, J. M., Li, Y., Lee, Y. J., Li, M., Brady, D. C., Di Toro, D. M., et al. (2014). Quantifying the effects of nutrient loading on dissolved O2 cycling and hypoxia in Chesapeake Bay using a coupled hydrodynamic-biogeochemical model. *Journal of Marine Systems*, *139*(March), 139–158. https://doi.org/10.1016/j.jmarsys.2014.05.018

Traving, S. J., Rowe, O., Jakobsen, N. M., Sørensen, H., Dinasquet, J., Stedmon, C. A., et al. (2017). The effect of increased loads of dissolved organic matter on estuarine microbial community composition and function. *Frontiers in Microbiology*, *8*(351), 1–15. https://doi.org/10.3389/fmicb.2017.00351

Trowbridge, P. (2010). *Analysis of Nitrogen Loading Reductions for Wastewater Treatment Facilities and Non-Point Sources in the Great Bay Estuary Watershed* (p. 35). Concord, NH: New Hampshire Department of Environmental Services. Retrieved from http://des.nh.gov/organization/divisions/water/wmb/coastal/documents/gb_nitro_load_analysis.pdf

Trowbridge, P, Wood, M., Underhill, J., & Healy, D. (2014). *Great Bay Nitrogen Non-Point Source Study. State of New Hampshire, Department of Environmental Services. 82pp.* State of New Hampshire Department of Environmental Services. Retrieved from https://www.google.com/url?sa=t&rct=j&q=&esrc=s&source=web&cd=1&cad=rja&uact=8&ved=0ahUKEwjJ67b4j9LLAhUCdT4KHUAZB4UQFggdMAA&url=http://des.nh.gov/organization/divisions/water/wmb/coastal/documents/gbnnpss-report.pdf&usg=AFQjCNF1lmoLE9VP_mPIldwya1X5VmBC6w&

Trowbridge, Phil. (2007). *Hydrologic Parameters for New Hampshire's Estuaries* (No. December). New Hampshire Department of Environmental Services,New Hampshire

Estuaries Project., Univ of New Hampshire., Durham. N.H. Retrieved from https://www.ntis.gov/Search/Home/titleDetail/?abbr=PB2011109624

Valiela, I., & Bowen, J. L. (2002). Nitrogen sources to watersheds and estuaries: Role of land cover mosaics and losses within watersheds. *Environmental Pollution*, *118*(2), 239–248. https://doi.org/10.1016/S0269-7491(01)00316-5

Vallino, J. J., Hopkinson, C. S., & Garritt, R. H. (2005). Estimating estuarine gross production, community respiration and net ecosystem production: A nonlinear inverse technique. *Ecological Modelling*, *187*(2–3), 281–296. https://doi.org/10.1016/j.ecolmodel.2004.10.018

Walling, D. E., & Webb, B. W. (1980). The spatial dimension in the interpretation of stream solute behaviour. *Journal of Hydrology*, *47*(1), 129–149. http://dx.doi.org/10.1016/0022-1694(80)90052-9

Wetz, M. S., & Yoskowitz, D. W. (2013). An 'extreme'future for estuaries? Effects of extreme climatic events on estuarine water quality and ecology. *Marine Pollution Bulletin*, *69*(1), 7–18.

Williams, G. P. (1989). Sediment concentration versus water discharge during single hydrologic events in rivers. *Journal of Hydrology*, *111*(1–4), 89–106. https://doi.org/10.1016/0022-1694(89)90254-0

Wollheim, W. M., Stewart, R. J., Aiken, G. R., Butler, K. D., Morse, N. B., & Salisbury, J. (2015). Removal of terrestrial DOC in aquatic ecosystems of a temperate river network. *Geophysical Research Letters*, *42*(16), 6671–6679. https://doi.org/10.1002/2015GL064647

Wollheim, Wilfred M., Pellerin, B. A., Vörösmarty, C. J., & Hopkinson, C. S. (2005). N retention in urbanizing headwater catchments. *Ecosystems*, *8*(8), 871–884. https://doi.org/10.1007/s10021-005-0178-3

Zorndt, A. C., Schlurmann, T., & Grabemann, I. (2012). The influence of extreme events on hydrodynamics and salinities in the Weser Estuary in the context of climate impact research. *Coastal Engineering Proceedings*, (33), 1–12. http://dx.doi.org/10.9753/icce.v33.currents.50

Figure and Table Captions

Figure 1 Map of Great Bay watershed showing land use, wastewater treatment plants (WWTP), sub-watersheds, sub-estuaries and water quality monitoring stations. Refer to Table 1 for summary land-use statistics.

Figure 2. (a) Time series of estuarine fDOM and watershed DOC fluxes from the Lamprey River in 2011. fDOM is reported in quinine sulfate equivalents parts per billion units (QSE ppb). **(b)** Time series of estuarine nitrate concentrations and watershed nitrate fluxes. Filtered signal refers to to removal of tide dominant frequencies.

Figure 3: Discharge hydrograph for the Lamprey River, with points identifying storms. Red markers are beginning or end of storm, and green markers represent the peak flow during a storm event. Additional variations in flow observed during summer dry periods were attributed to water releases done in an upstream reservoir as part of a construction and maintenance project.

Figure 4 *Frequency dependent coherence* between estuarine NO_3, fDOM and chloride with, (a) watershed discharge, (b) respective watershed concentrations (NO_3, fDOM and chloride), and (c) respective watershed fluxes (NO_3, DOC and chloride. Increasing time scales are from right to left with some highlighted.

Figure 5 Hysteresis patterns between estuarine concentrations and watershed fluxes for storm events between April and November 2011 **(a)** DOC, **(b)** Cl, **(c)** NO_3. and **(d)** inset plot showing NO_3 response to less intense storms. Storm events are indicated at the beginning of each storm as per their description in Table 2.

Figure 6 Relationship between baseflow watershed fluxes just prior to beginning of a storm event and corresponding estuarine concentration (a) NO_3 (b) estuarine fDOM and watershed DOC, and (c) Chloride.

Figure 7. Relationship between estuarine responsiveness (α) for NO3 with (a) storm event duration (b) total storm runoff (c) total storm precipitation.

Figure 8. Relationship between estuarine responsiveness (α) for fDOM with (a) storm event duration (b) total storm runoff (c) total storm precipitation.

Figure 9. Relationship between estuarine responsiveness (α) for Cl with (a) storm event duration (b) total storm runoff (c) total storm precipitation.

Table 1: Land use statistics for the Great Bay watershed and its major sub-watersheds

Table 2. Storm characteristics and patterns between estuarine and watershed NO3, terrestrial DOC and Cl for 13 storm events monitored.

Table 3: Average coherence values over time scales larger than a day .

Table 1: Land use statistics for the Great Bay watershed and its major sub-watersheds

Watershed	Total Area km^2	Developed Land (km^2) (%)	Agricultural Land (km^2) (%)	Forests and Wetlands (km^2) (%)	Water (km^2) (%)	Remarks
Great Bay	2652.5	369.9(14.0)	202.5(7.6)	1976.6 (74.5)	103.4 (3.9)	Whole watershed
Bellamy River	87.9	16.7 (19.0)	8.7 (9.8)	58.2 (66.2)	4.4 (5.0)	
Cocheco River	479.8	74.4 (15.5)	34.5 (7.2)	359 (74.8)	12 (2.5)	
Lamprey River	555.0	55.8 (10.1)	32.7 (5.9)	456.3 (82.2)	10.3 (1.9)	Sub-watershed monitored in this study
Oyster River	79.1	17.7(22.4)	9.1 (11.5)	50.5 (63.9)	1.8 (2.3)	
Salmon Falls River	852.6	84.5 (9.9)	57.8 (6.8)	686.1 (80.5)	24.2 (2.8)	
Squamscott/Exeter River	330.6	47.7 (14.4)	40.1 (12.1)	239 (72.3)	3.9 (1.2)	
Winnicut River	48.1	14.0 (29.2)	5.2 (10.8)	28.3 (58.7)	0.7 (1.4)	
Great Bay Drainage	70.6	10.6 (15.0)	6.7 (9.5)	30.3 (43.0)	23 (32.5)	Direct drainage to Great Bay proper
Lower Piscataqua Drainage	147.4	48.5 (32.9)	7.7 (5.2)	67.9 (46.0)	23.3 (15.8)	Direct drainage to Piscataqua River

Table 2. Storm characteristics and patterns between estuarine and watershed NO3, terrestrial DOC and Cl for 13 storm events monitored..

						Estuary-fDOM Vs Watershed DOC fluxes					Estuary NO_3 Vs. Watershed NO_3 fluxes					Estuary Cl Vs. Watershed Cl Fluxes
Storm No	Begin Date (mm-dd)	Storm Duration (days)	Mean Flow (m^3/s)	Total Storm Vol. (m3 /10^3)	Total Precip.[c] (mm)	Rising Limb fit, α [z]	p-value	Falling Limb fit, α [z]	p-value	Hyst. Pattern [a]	Rising Limb fit, α [z]	p-value	Falling Limb fit, α [z]	p-value	Hyst. Pattern [a]	Hyst. Pattern [a]
1	05-14	21	16.2	12614	95	0.13	0.000	0.15	0.000	AC	0.51	0.000	-0.01	0.357	AC	C
2	06-09	12	4.5	621	56	-0.01	0.087	0.15	0.000	AC	0.55	0.000	1.23	0.000	AC	C
3	06-22	14	6.6	3183	57	0.09	0.000	0.14	0.000	AC	0.34	0.000	0.06	0.000	ML	C
4	08-08	7	0.8	186	23	-0.02	0.051	-0.04	0.000	ML	-0.08	0.000	0.64	0.000	ML	ML
5	08-15	9	1.8	769	54	0.00	0.267	-0.07	0.000	AC	0.22	0.000	0.01	0.000	AC	C
6	08-24	13	5.7	3911	92	0.06	0.000	0.07	0.000	AC	0.13	0.000	-0.15	0.000	AC	C
7	09-06	11	4.0	1303	47	0.11	0.000	0.09	0.000	AC	0.03	0.083	0.25	0.000	ML	C
8	09-23	6	3.1	545	38	-0.04	0.000	0.21	0.000	C[b]	-0.12	0.000	-0.11	0.000	AC	AC
9	09-29	13	10.6	7232	95	0.40	0.000	0.00	0.294	AC	0.13	0.000	0.17	0.000	ML	C
10	10-13	6	11.5	2778	56	-0.02	0.000	-0.28	0.000	AC	0.41	0.000	0.01	0.231	ML	C
11	10-19	8	13.1	3507	67	0.01	0.057	0.05	0.000	AC	0.01	0.108	-0.13	0.000	AC	C
12	10-27	14	15.1	7011	58	-0.02	0.000	0.22	0.000	AC	0.11	0.000	0.29	0.000	ML	C
13	11-09	13	15.9	5751	69	-0.03	0.004	NA	0.000	NA[c]	0.10	0.000	NA	0.000	NA	NA

Notes Hysteresis Patterns (Hyst.Pattern) : AC- Anti-Clockwise , C-Clockwise, ML-Multi-Loop.

[z]- fit parameter for equation $P = b * F^{\alpha}$

NA-Not Available, [c]precipitation recorded at nearby National Weather Service Station in Durham,NH

Table 3: Average coherence values over time scales larger than a day .

		Watershed Variable						
		Q	NO_3	DOC	Cl	NO_3 flux	DOC flux	Cl flux
Estuarine Constituent	NO_3	0.21	0.049			0.133		
	fDOM	0.217		0.087			0.208	
	Cl	0.171			0.107			0.157

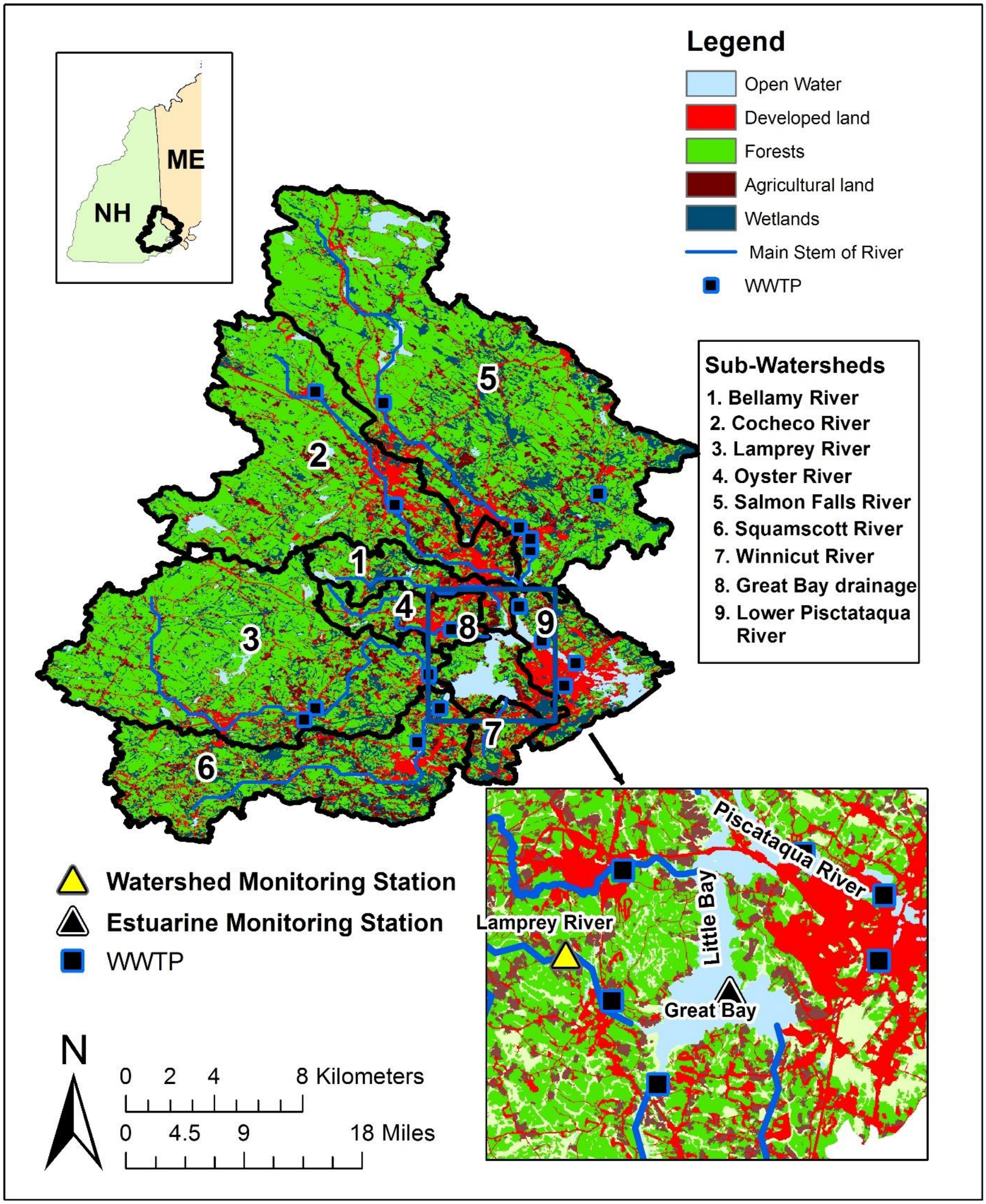

Figure 1: Map of Great Bay watershed showing land use, wastewater treatment plants (WWTP), sub-watersheds, sub-estuaries and water quality monitoring stations. Refer to Table 1 for summary land-use statistics.

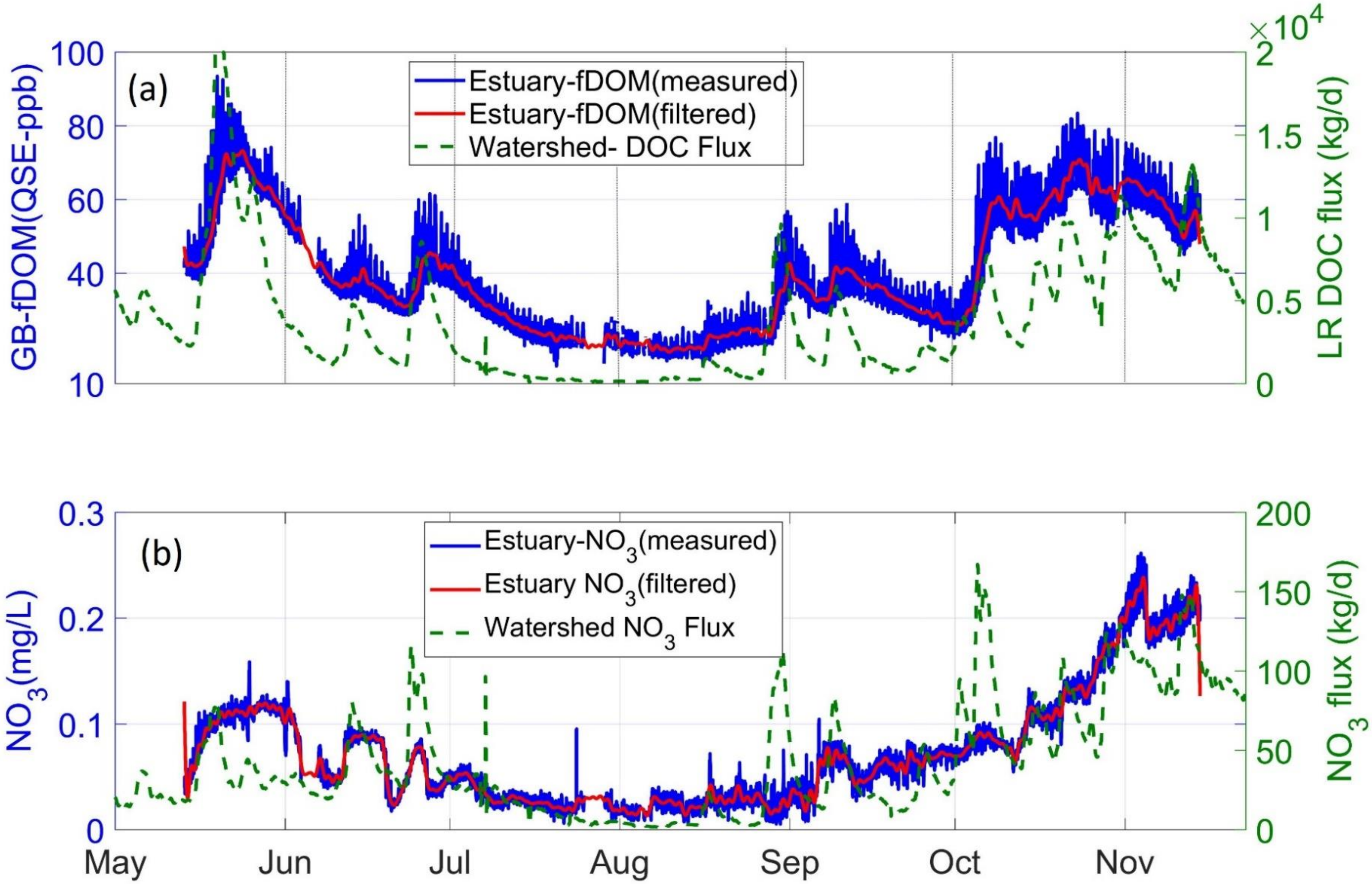

Figure 2: (a) Time series of estuarine fDOM and watershed DOC fluxes from the Lamprey River in 2011. fDOM is reported in quinine sulfate equivalents parts per billion units (QSE ppb). **(b)** Time series of estuarine nitrate concentrations and watershed nitrate fluxes. Filtered signal refers to to removal of tide dominant frequencies.

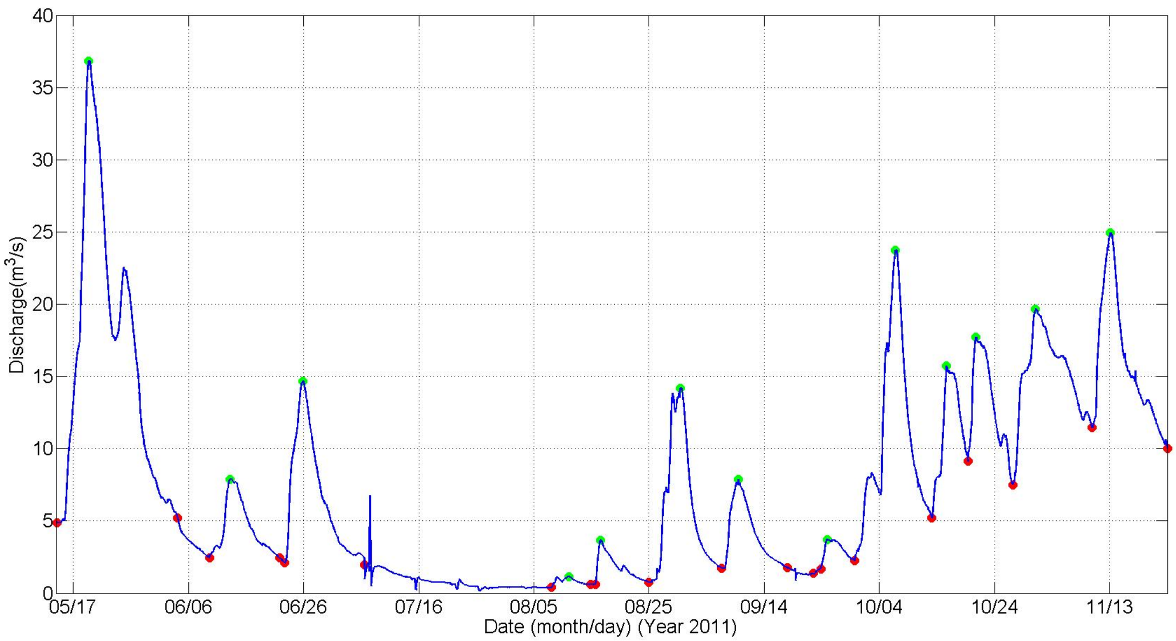

Figure 3: Discharge hydrograph for the Lamprey River, with points identifying storms. Red markers are beginning or end of storm, and green markers represent the peak flow during a storm event. Additional variations in flow observed during summer dry periods were attributed to water releases done in an upstream reservoir as part of a construction and maintenance project.

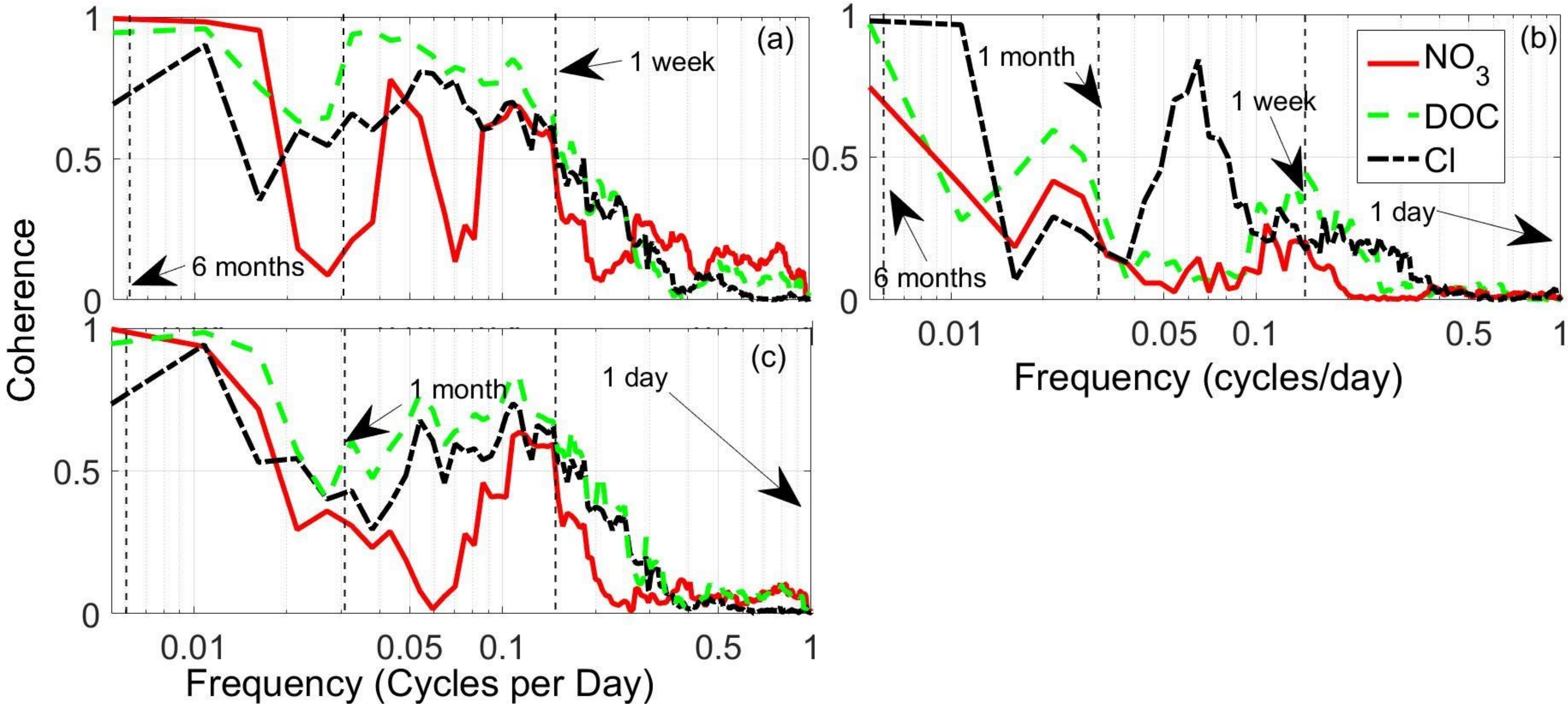

Figure 4: *Frequency dependent coherence* between estuarine NO_3, fDOM and chloride with, (a) watershed discharge, (b) respective watershed concentrations (NO_3, fDOM and chloride), and (c) respective watershed fluxes (NO_3, DOC and chloride. Increasing time scales are from right to left with some highlighted.

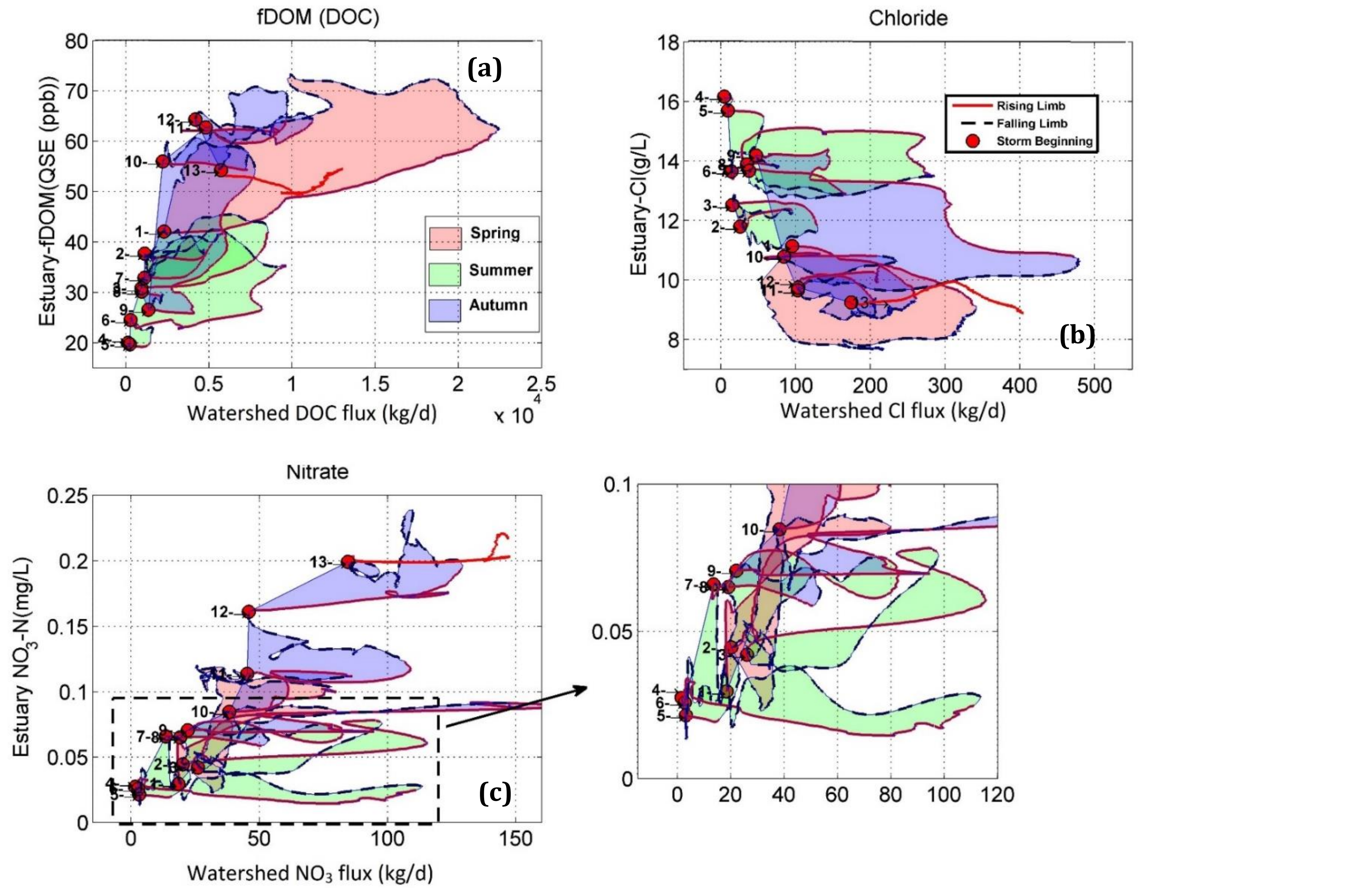

Figure 5: Hysteresis patterns between estuarine concentrations and watershed fluxes for storm events between April and November 2011 **(a)** DOC, **(b)** Cl, **(c)** NO_3. and **(d)** inset plot showing NO_3 response to less intense storms. Storm events are indicated at the beginning of each storm as per their description in Table 2.

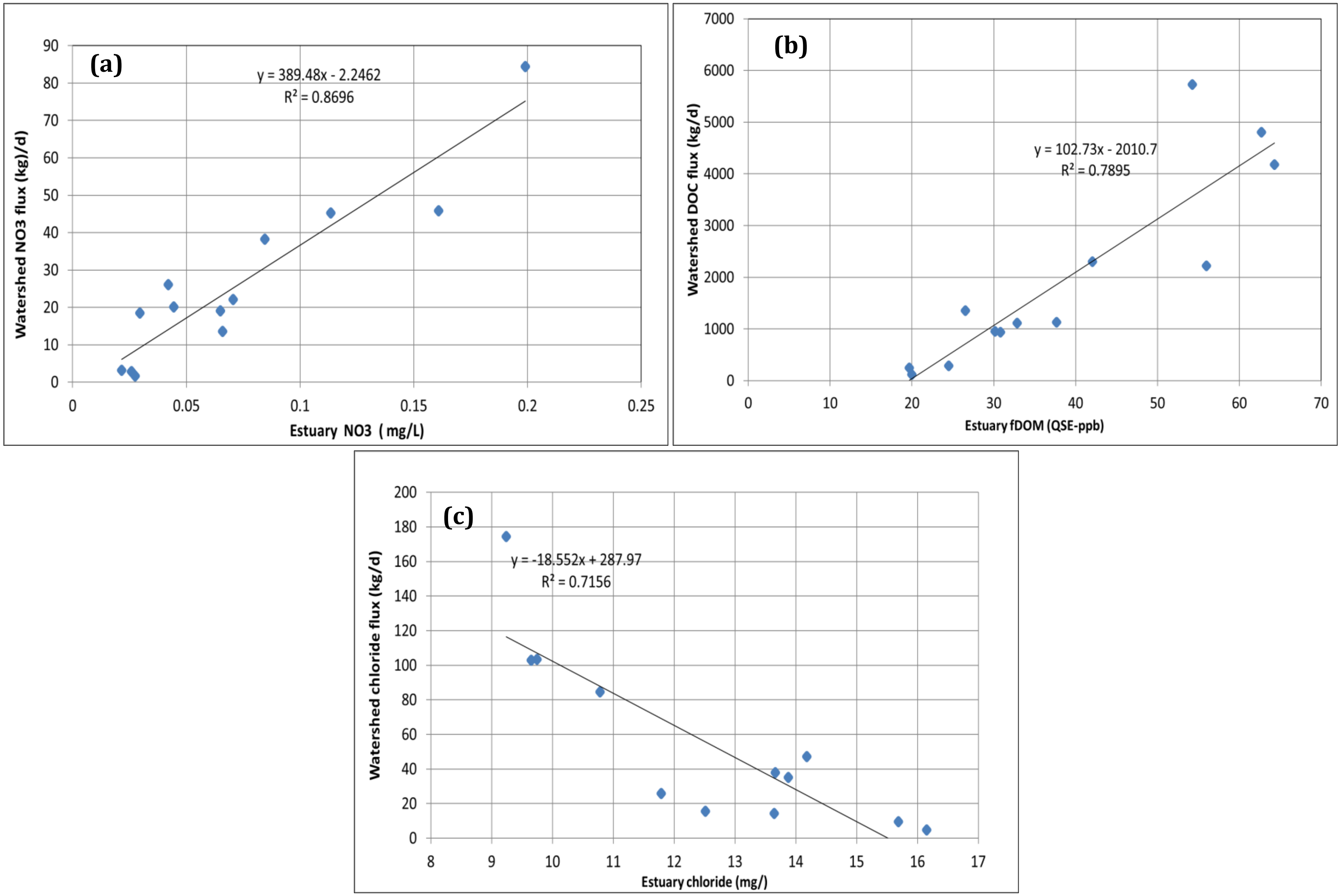

Figure 6 Relationship between baseflow watershed fluxes just prior to beginning of a storm event and corresponding estuarine concentration (a) NO_3 (b) estuarine fDOM and watershed DOC, and (c) chloride.

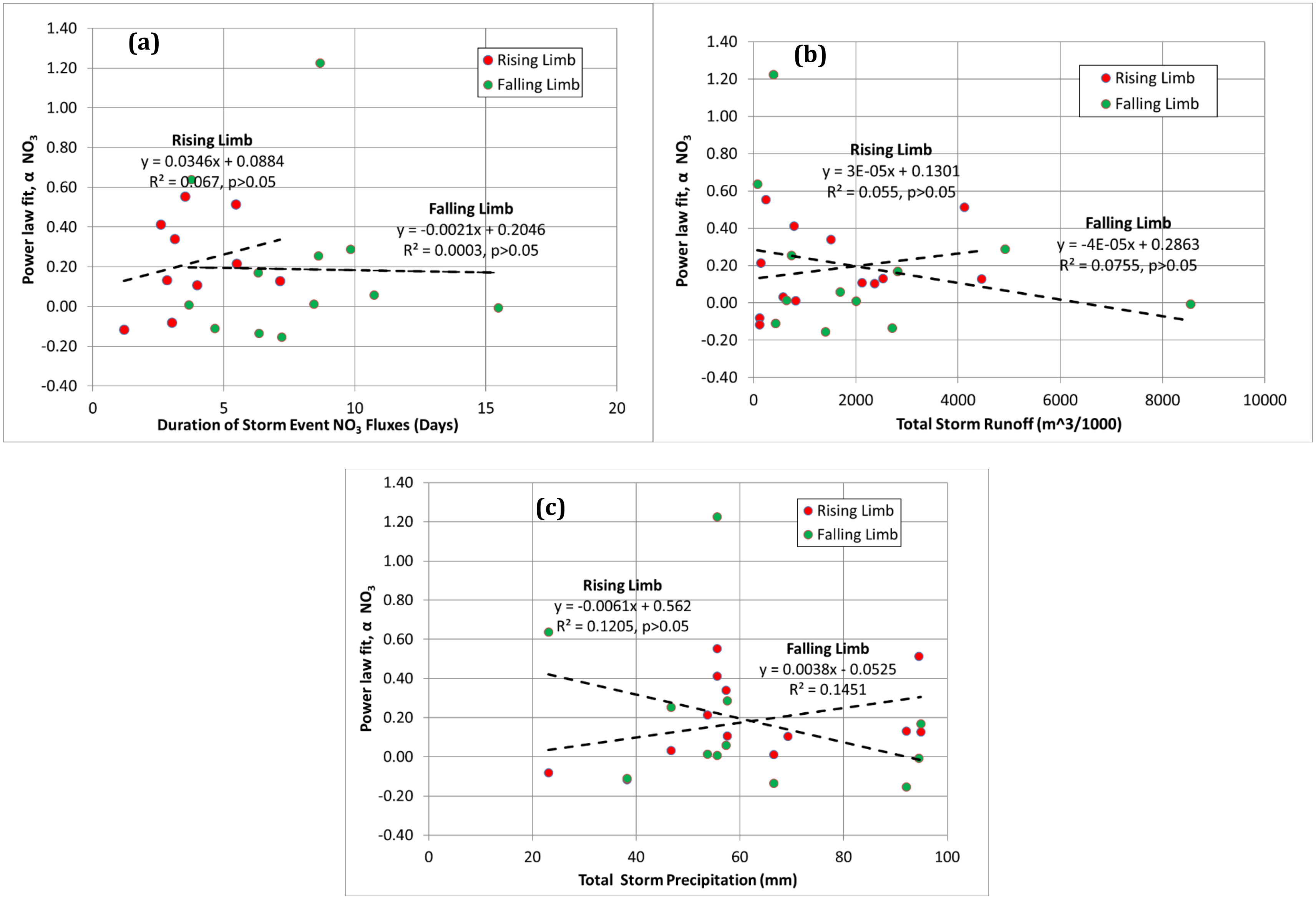

Figure 7. Relationship between estuarine responsiveness (α) for NO_3 with (a) storm event duration (b) total storm runoff (c) total storm precipitation.

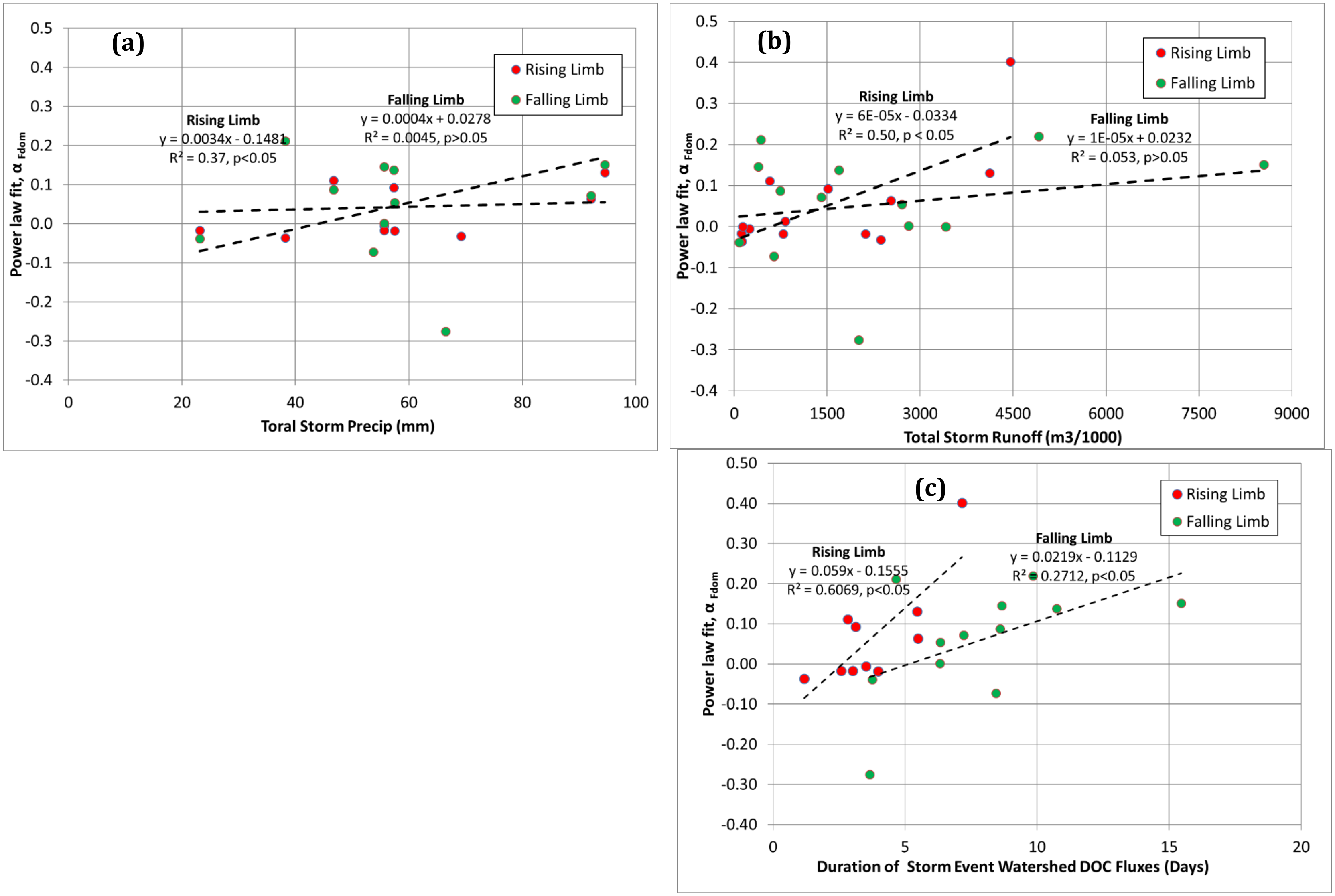

Figure 8. Relationship between estuarine responsiveness (α) for fDOM with (a) storm event duration (b) total storm runoff (c) total storm precipitation

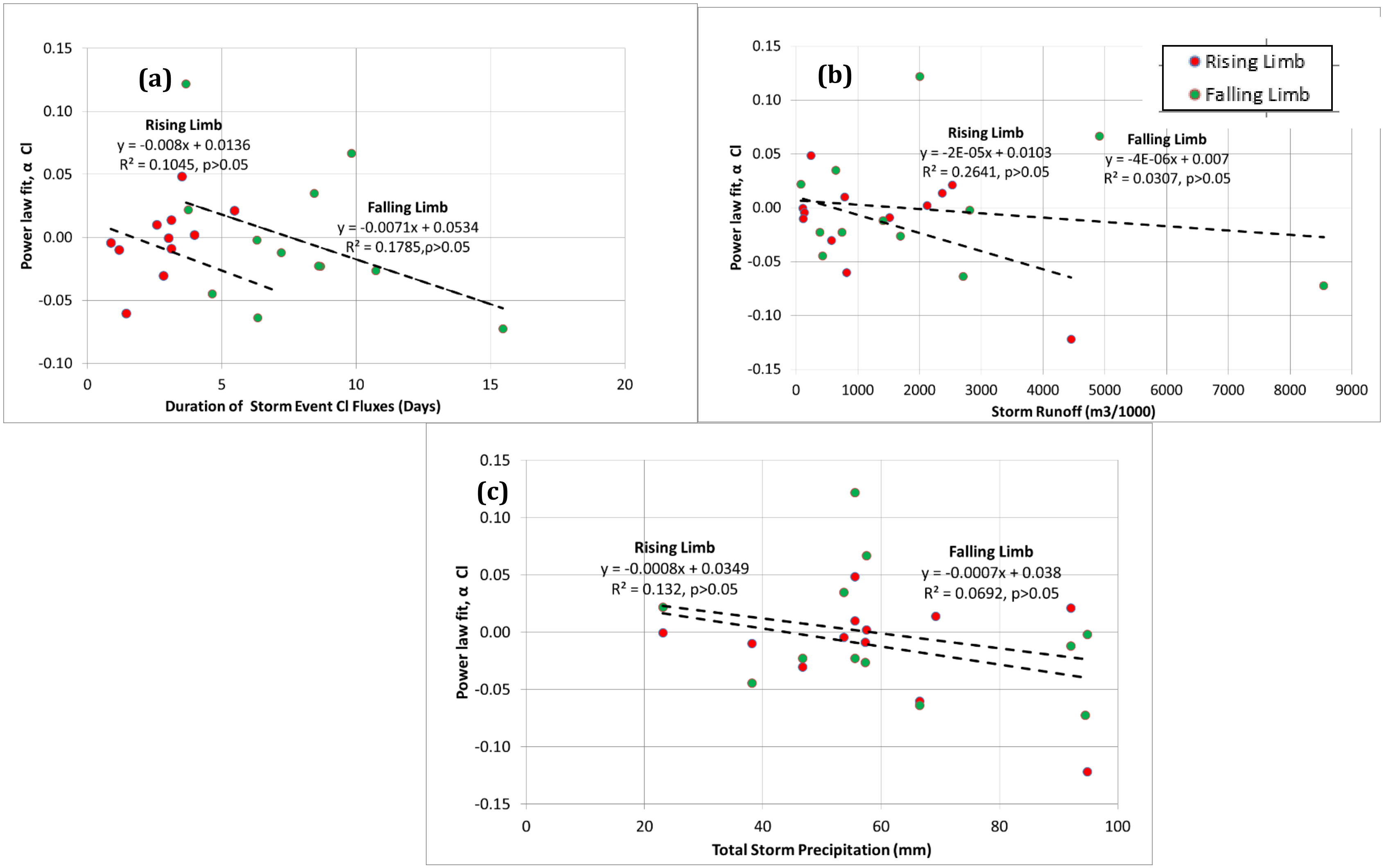

Figure 9. Relationship between estuarine responsiveness (α) for Cl with (a) storm event duration (b) total storm runoff (c) total storm precipitation.

Supporting Information for

High frequency concurrent measurements in watershed and impaired estuary reveal coupled DOC and decoupled nitrate dynamics.

Gopal K. Mulukutla [1], Wilfred M.Wollheim[1,2], Joseph E. Salisbury[3], Richard O. Carey[1,2], Thomas K .Gregory[3] and William H. McDowell[2]

[1]Earth Systems Research Center, University of New Hampshire, Durham, New Hampshire, USA.

[2]Department of Natural Resources and the Environment, University of New Hampshire, Durham, New Hampshire, USA

[3]Ocean Processes Analysis Laboratory, University of New Hampshire, Durham, New Hampshire, USA

Supporting Information Content

Text S1 to S2
Table S1
Figures S1 to S13

Dataset file (csv file)
Dataset Metadata file (text file)

Introduction

This document describes residence time estimates of the Great Bay estuary, data pre-processing performed to determine lag in time series.

Table1 provides information on

- Lag measured between storm event watershed DOC fluxes and estuarine fDOM

Figures S1-S13 provide information on

- Individual storm event hysteresis response of estuarine fDOM, Cl and NO_3 to respective watershed fluxes

Supporting Dataset and Metadata

- A comma separated (csv) file containing the underlying data
- A text file containing the description of variables, and related information about the datafile

Text S1 Residence Times in the Great Bay Estuarine System

There are various ways to characterize the tide driven removal of water and constituents from an estuary.

(a) **Flushing time** is the time taken to remove a constituent by a pre-determined factor from a region of the estuary (Aikman & Lanerolle, 2005; Bilgili et al., 2005) used a numerical circulation model to determine the time taken for a 63 % reduction in a conservative tracer from each sub-estuary in the system. They found that with river inputs at average annual rates the flushing time was 9.2 days for the Great Bay sub-estuary, as opposed to 29.1 days for the estuarine system as a whole.

(b) Residence time is the time taken by a parcel of water to be removed from the boundaries of a specific region (Aikman & Lanerolle, 2005; Bilgili et al., 2005)estimated that it took 19.6 days for a water parcel to exit the Great Bay sub-estuary with rivers inputs at average annual conditions.

Text S2 Lag in time series

The application of a commonly used method to determine lag (cross correlation)(Menke & Menke, 2012)) did not yield consistent results for nine of the thirteen storm events (see e.g. Table S1). We attribute this to be largely due to "noisiness" in estuarine time series data, an artifact of the filtering procedure applied in removing tidal frequencies. Thus, we did not correct our data for lag. However, this does not affect the results of coherence analysis, as all the frequencies within the signal are considered in the analysis, and results are in frequency domain.

The lack of lag correction may affect the "power-law" analysis of storm event time series (results of watershed-estuary coupling in storm event time scales). We determined two areas where this could affect the results – (a) lag in storm event time series may result incorrect input of rising limb or falling limb data., and (b) lack of alignment in peaks (e.g. between watershed fluxes and estuarine concentrations) may result in increased uncertainty in determination of estuarine responsiveness (α). Based on data from four of the thirteen storm event, the length of lag as a fraction of the total duration of the storm event was small (Table S1). This suggests that error associated with (a) will be minimal and for (b) it will not affect the overall weight of the results. Characterization of the uncertainty related to the lack of lag correction will require the collection of data for more storm events.

Table S1: Lag measured between storm event watershed DOC fluxes and estuarine fDOM

Storm Duration (days)	Lag (days)	Lag as a fraction of storm duration (%)
20.9	1.3	6.3
12.2	-	-
13.9	0.9	6.3
6.8	-	-
9.3	-	-
12.7	1.4	11.5
11.4	-	-
5.8	-	-
13.5	1.0	7.4
6.3	-	-
7.8	-	-
13.8	-	-
13.1	-	-

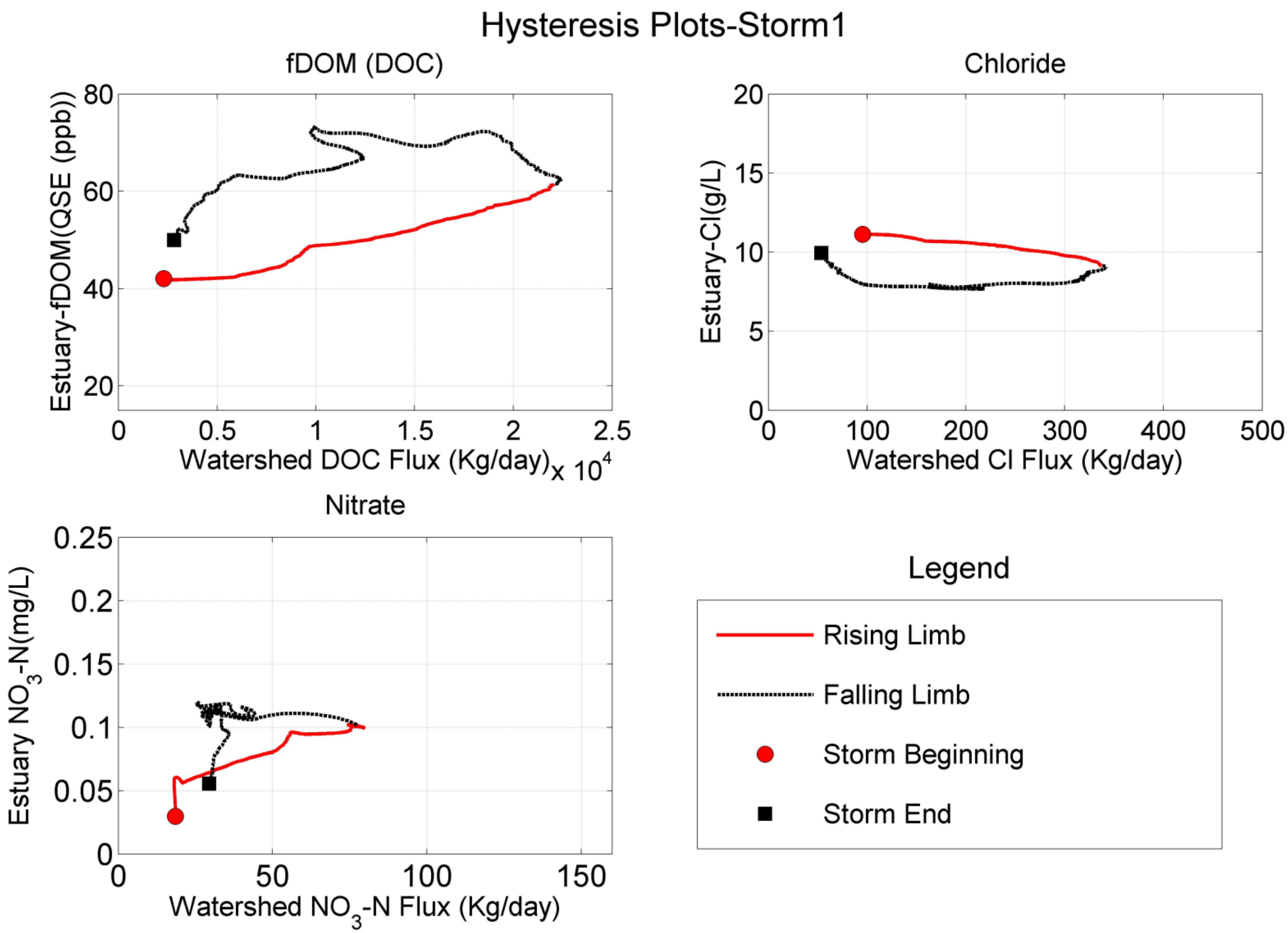

Figure S1 Hysteresis Pattern for one storm event, watershed variable (fluxes of DOC, NO3, and Cl) Vs. Estuarine variable (fDOM, NO3, Cl)

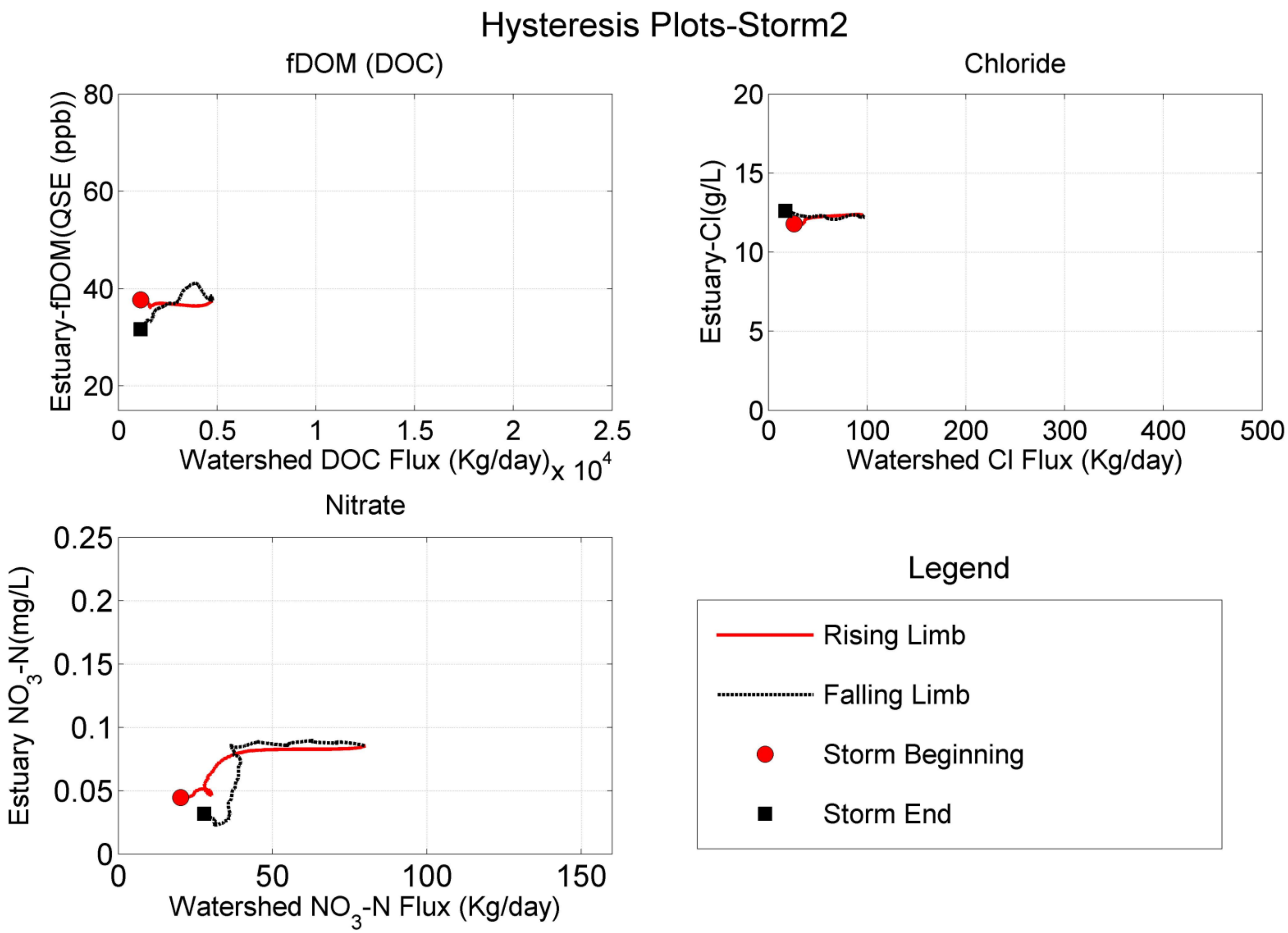

Figure S2 Hysteresis Pattern for one storm event, watershed variable (fluxes of DOC, NO3-N, and Cl) Vs. Estuarine variable (fDOM, NO3, Cl)

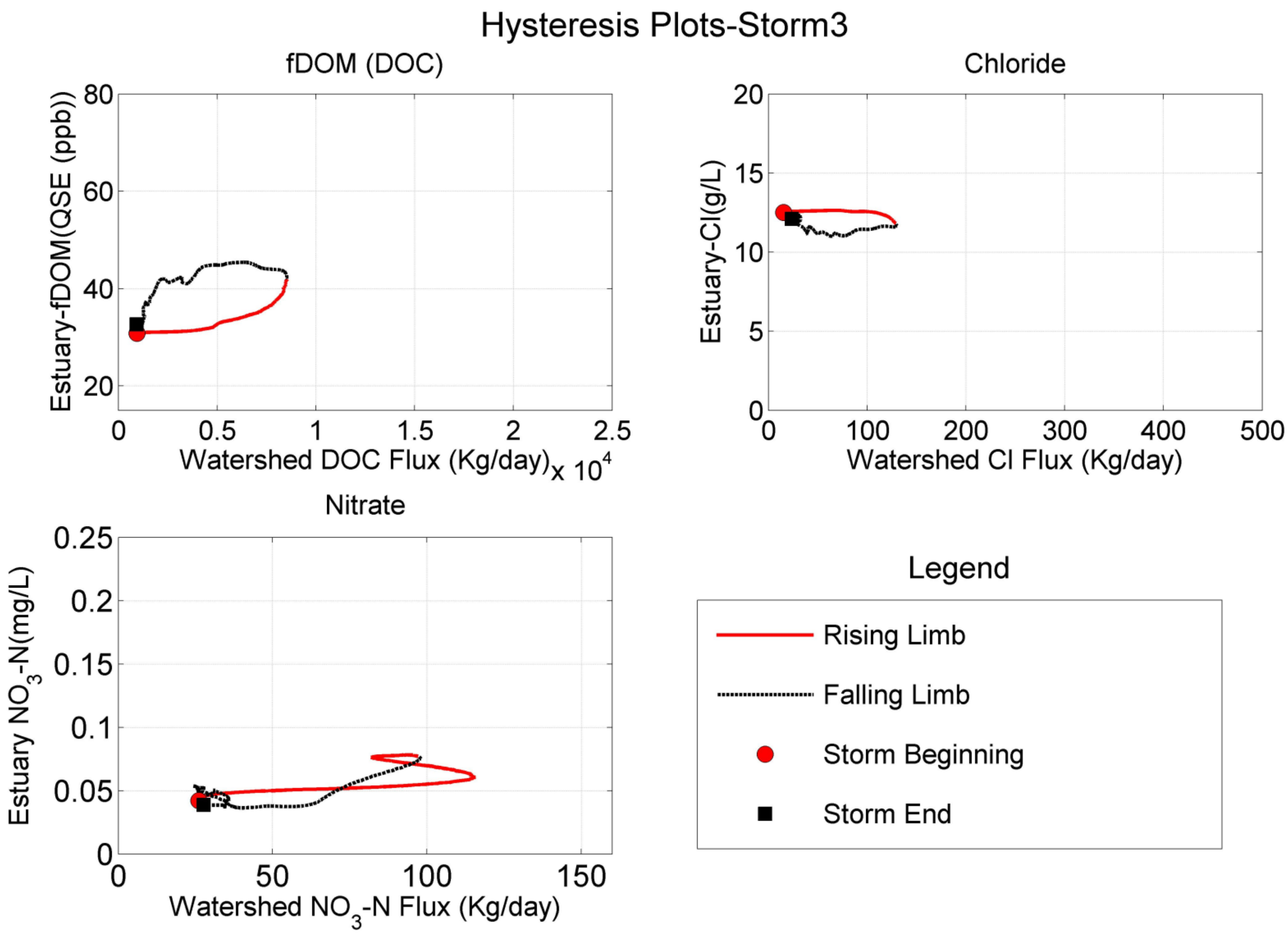

Figure S3 Hysteresis Pattern for one storm event, watershed variable (fluxes of DOC, NO_3 , and Cl) Vs. Estuarine variable (fDOM, NO3, Cl)

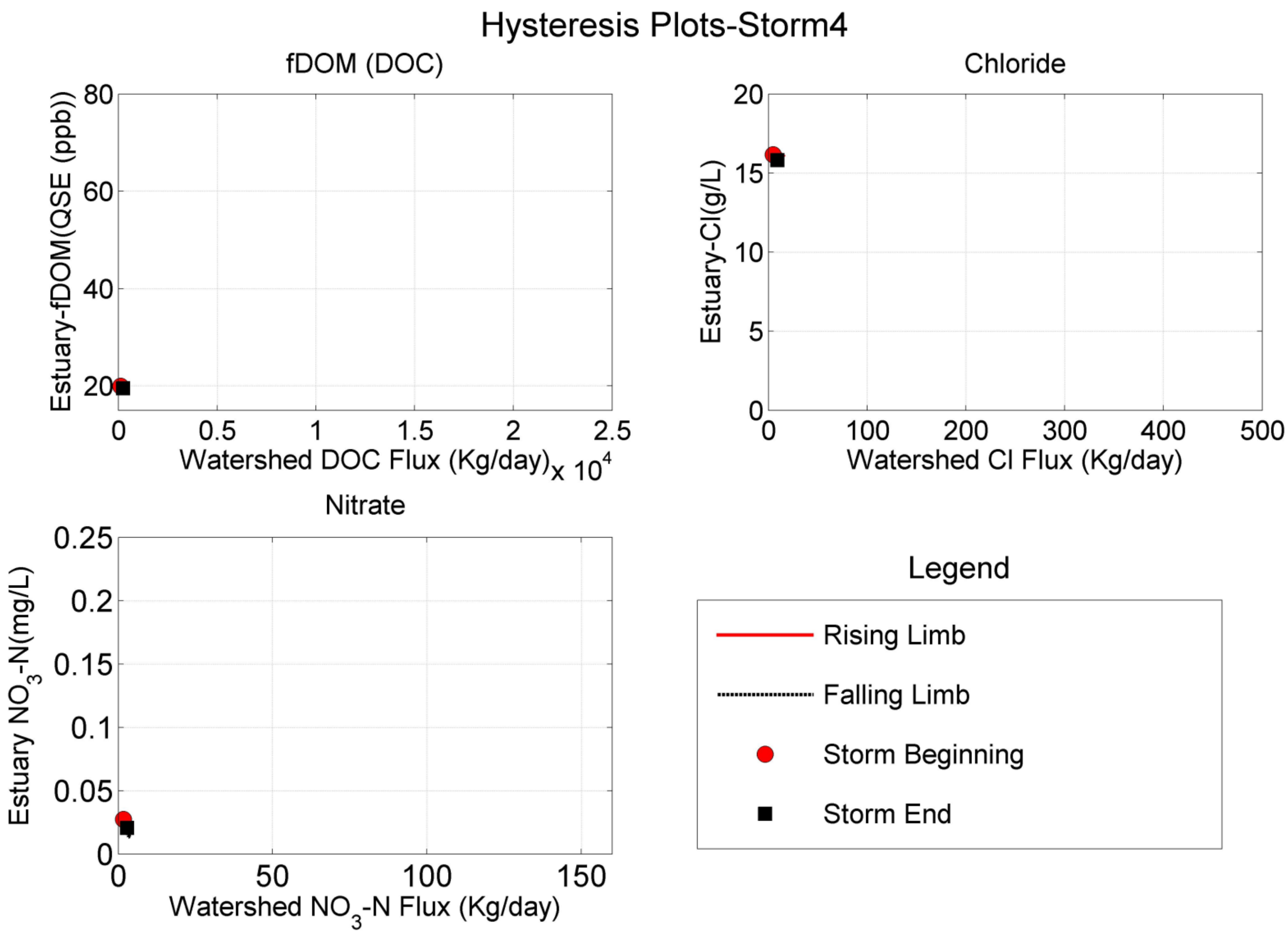

Figure S4 Hysteresis Pattern for one storm event, watershed variable (fluxes of DOC, NO_3 , and Cl) Vs. Estuarine variable (fDOM, NO3, Cl)

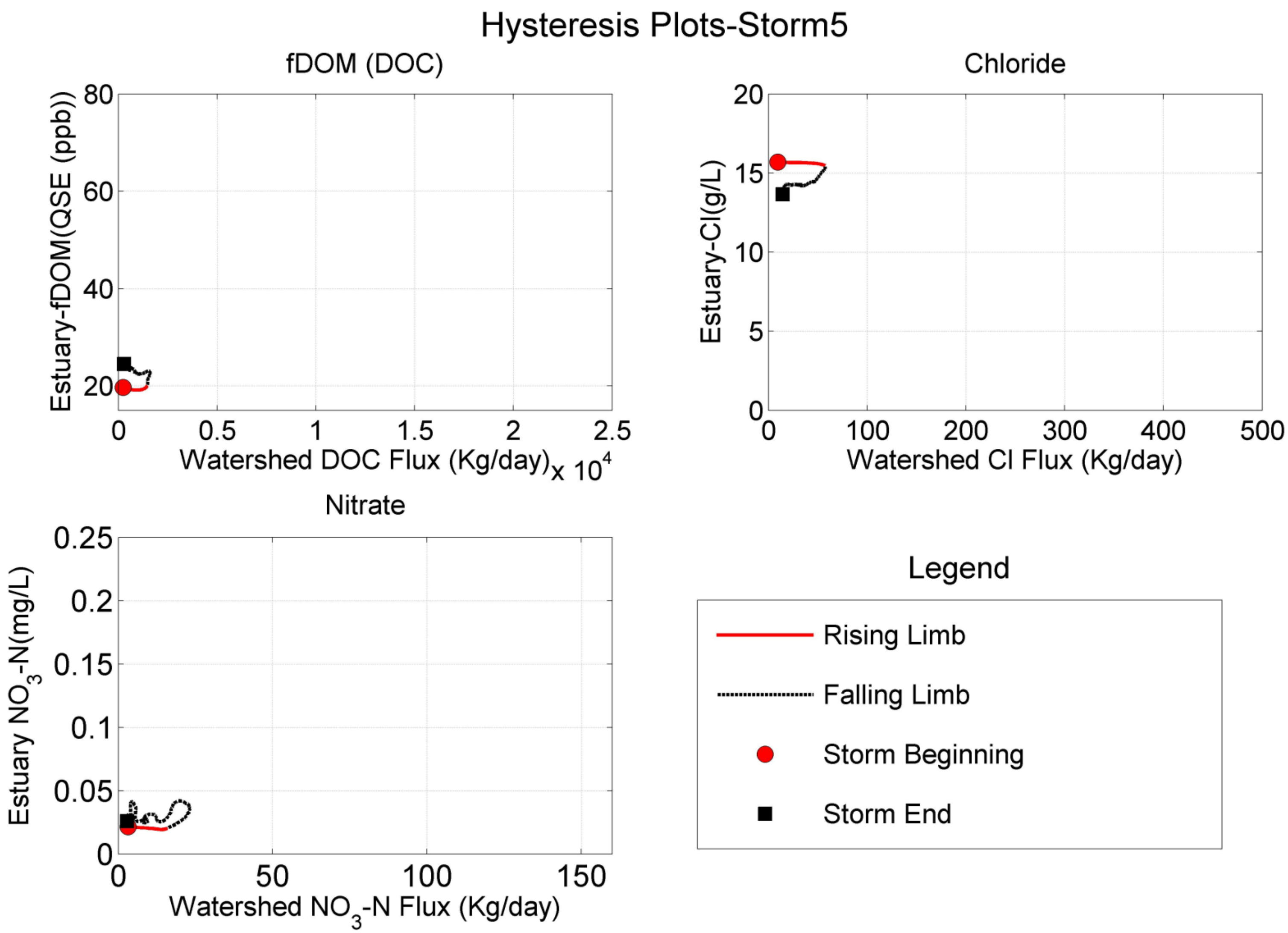

Figure S5 Hysteresis Pattern for one storm event, watershed variable (fluxes of DOC, NO_3 , and Cl) Vs. Estuarine variable (fDOM, NO3, Cl)

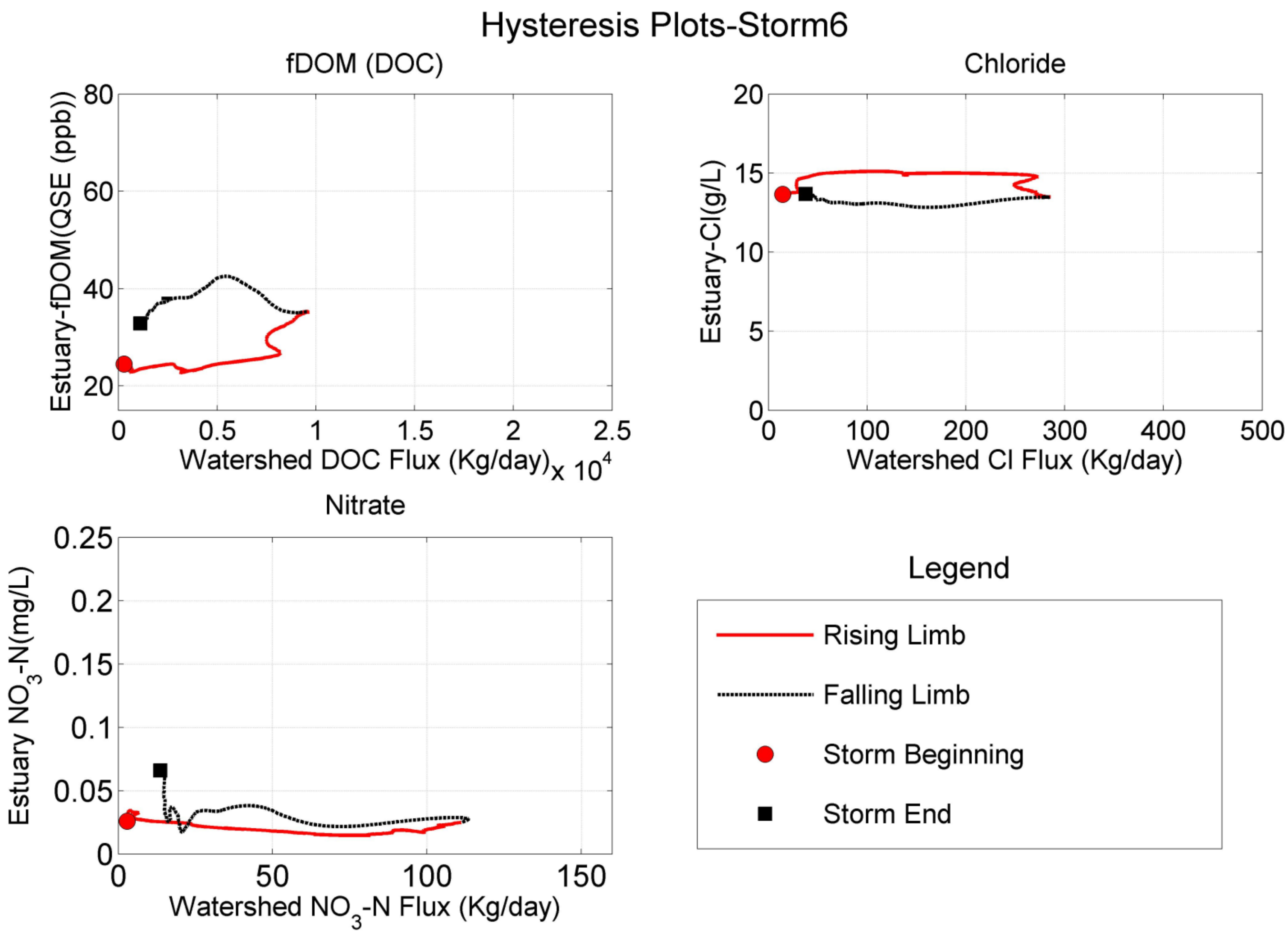

Figure S6 Hysteresis Pattern for one storm event, watershed variable (fluxes of DOC, NO_3, and Cl) Vs. Estuarine variable (fDOM, NO3, Cl)

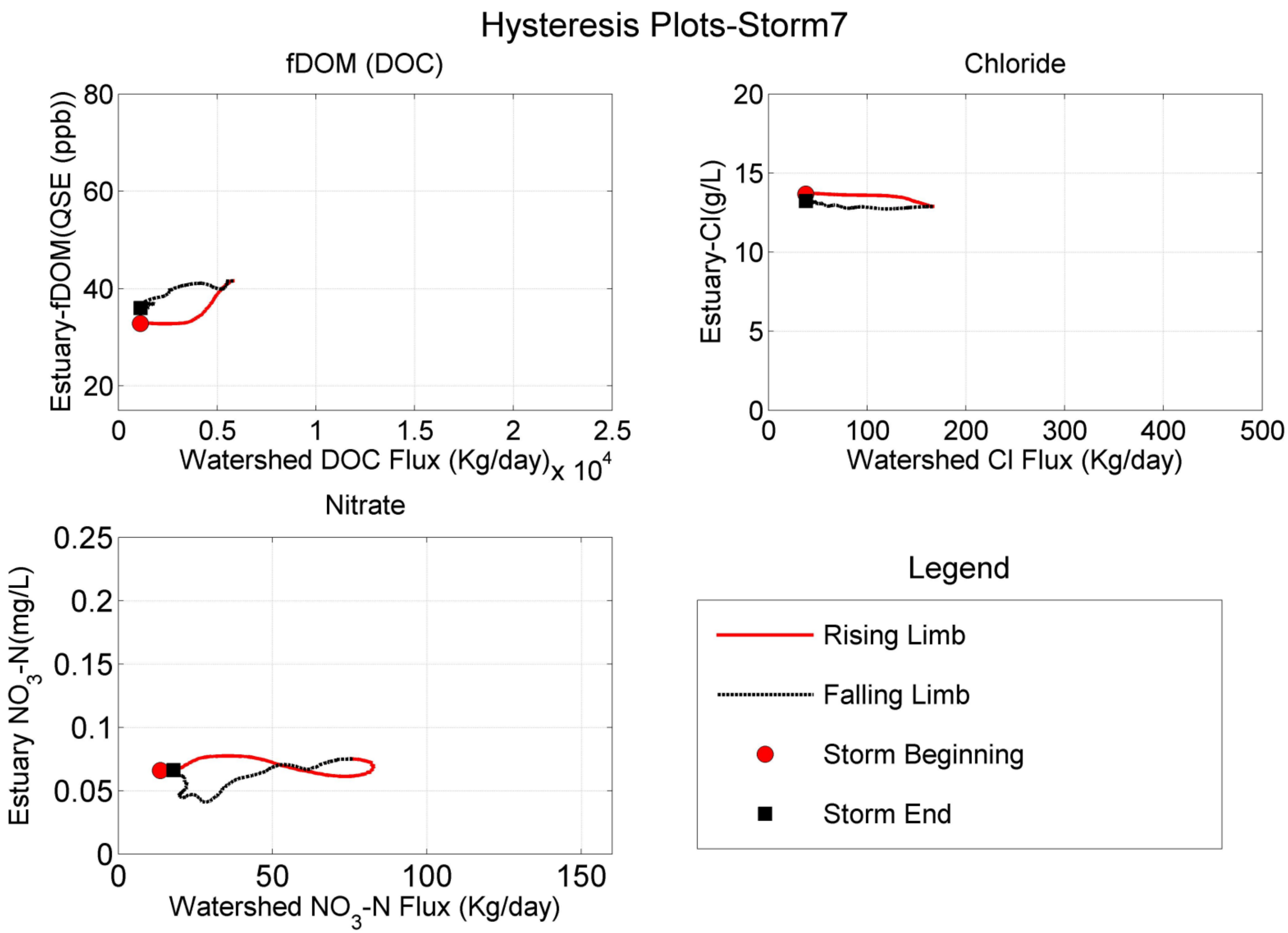

Figure S7 Hysteresis Pattern for one storm event, watershed variable (fluxes of DOC, NO_3 , and Cl) Vs. Estuarine variable (fDOM, NO3, Cl)

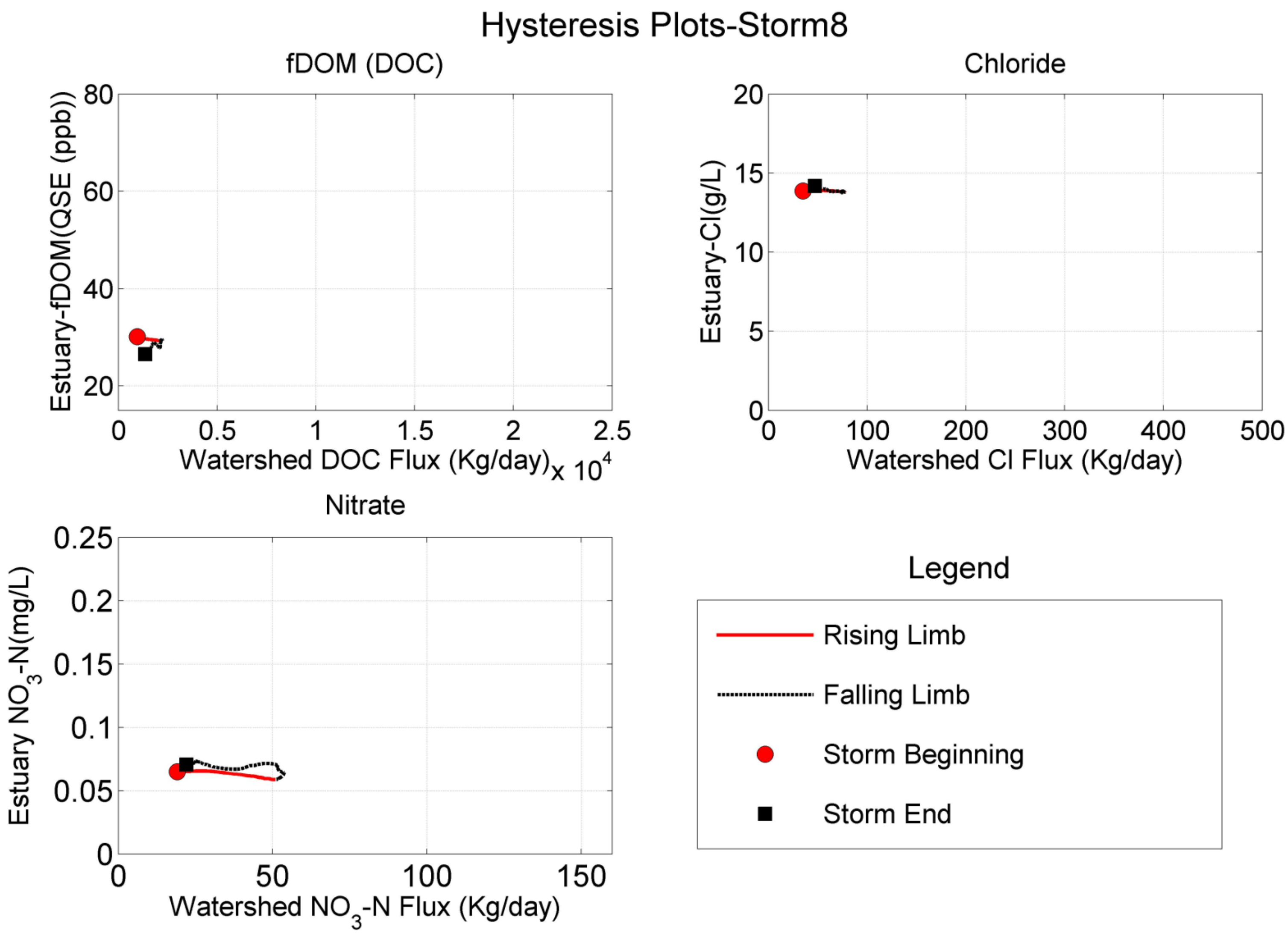

Figure S8 Hysteresis Pattern for one storm event, watershed variable (fluxes of DOC, NO_3 , and Cl) Vs. Estuarine variable (fDOM, NO3, Cl)

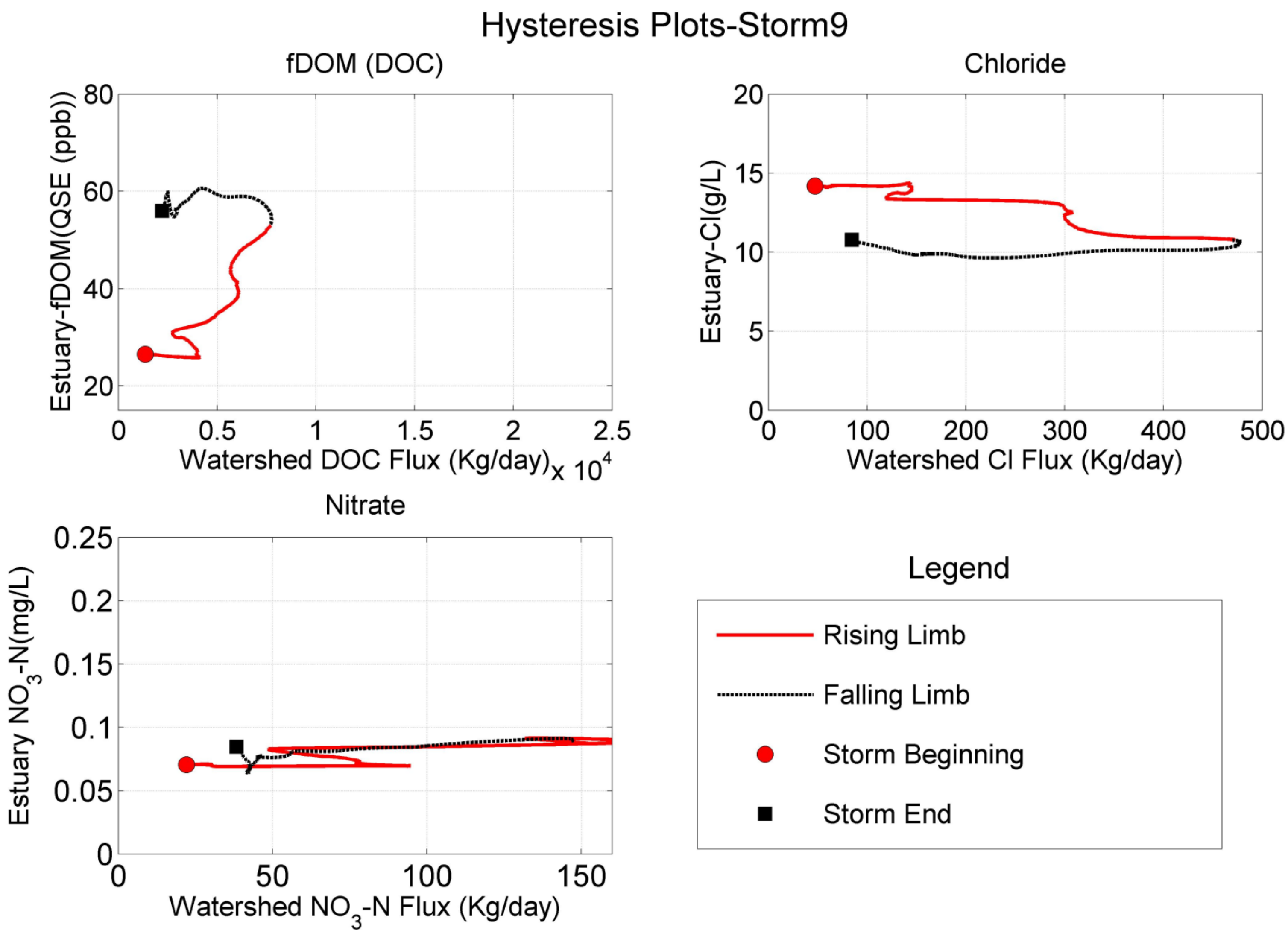

Figure S9 Hysteresis Pattern for one storm event, watershed variable (fluxes of DOC, NO_3 , and Cl) Vs. Estuarine variable (fDOM, NO3, Cl)

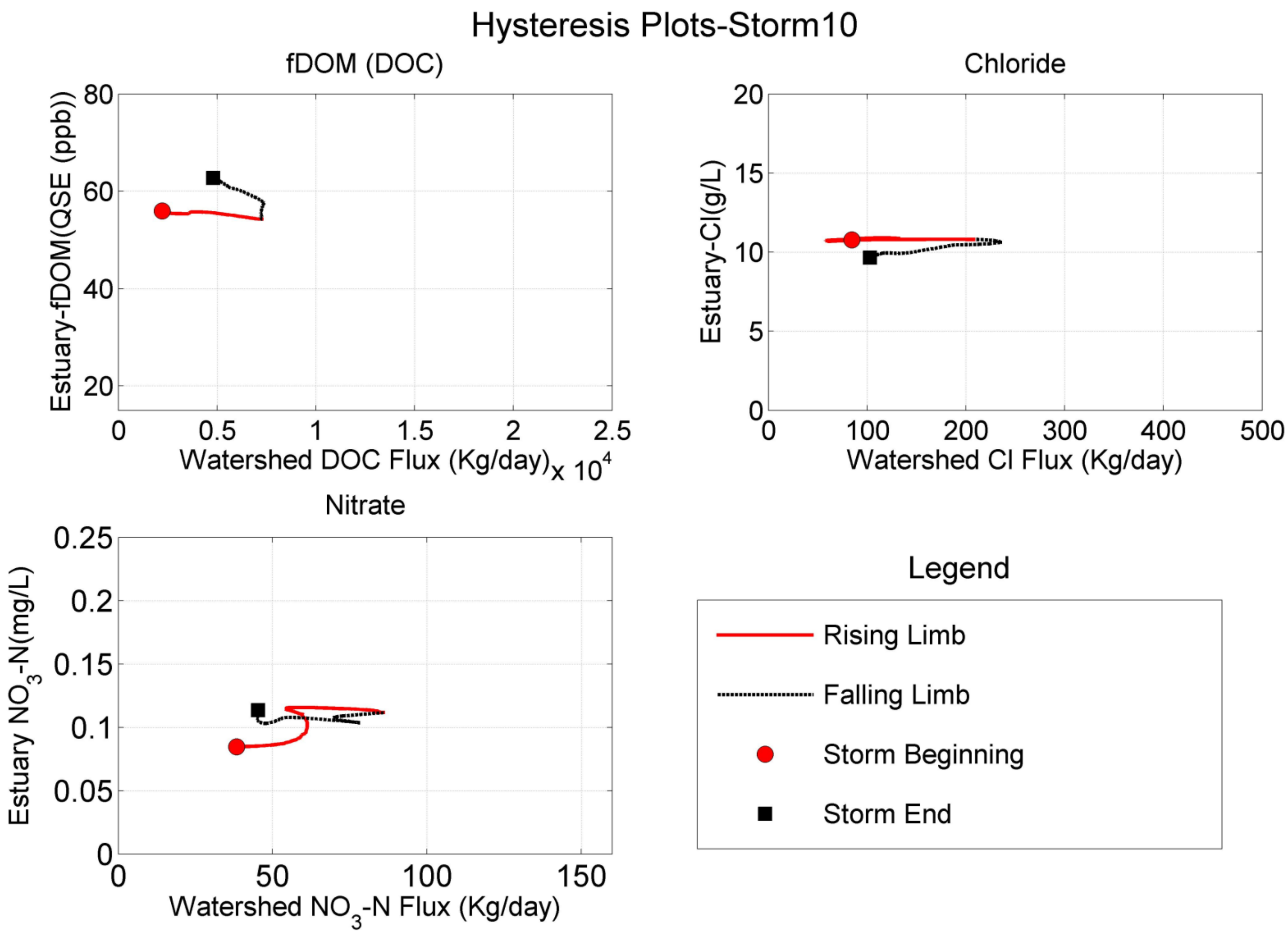

Figure S10 Hysteresis Pattern for one storm event, watershed variable (fluxes of DOC, NO_3 , and Cl) Vs. Estuarine variable (fDOM, NO3, Cl

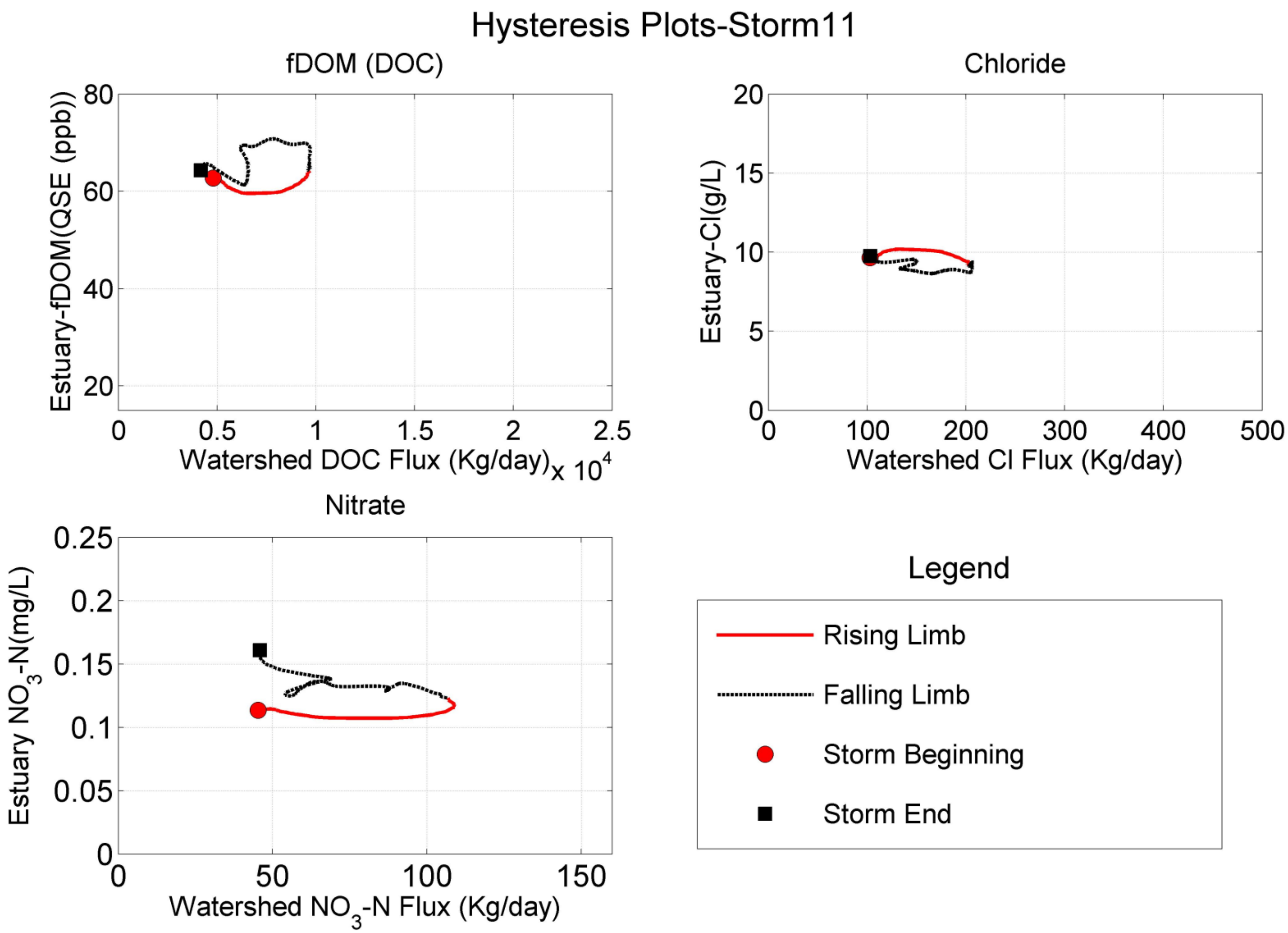

Figure S11 Hysteresis Pattern for one storm event, watershed variable (fluxes of DOC, NO_3 , and Cl) Vs. Estuarine variable (fDOM, NO_3, Cl)

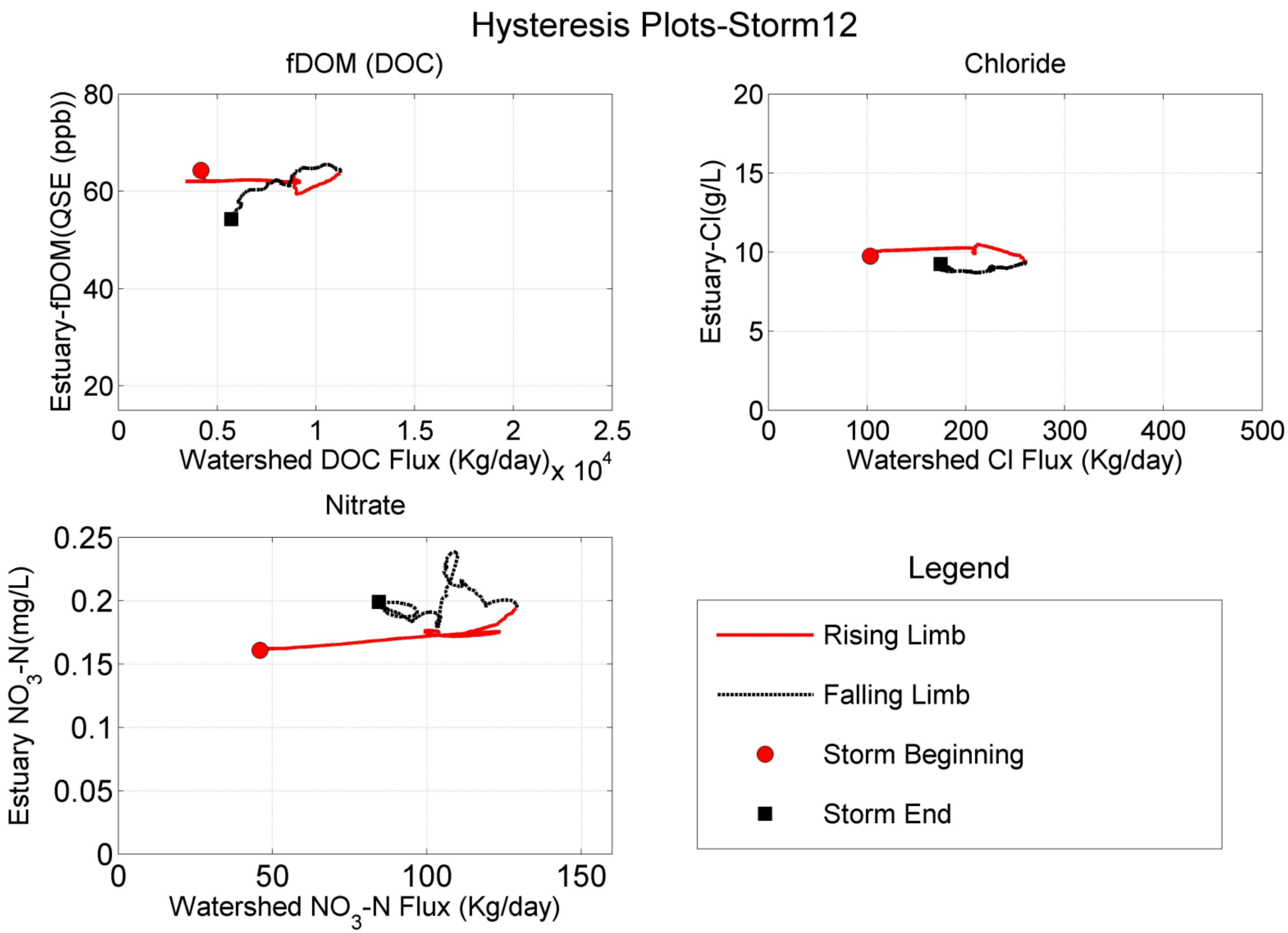

Figure S12 Hysteresis Pattern for one storm event, watershed variable (fluxes of DOC, NO_3 , and Cl) Vs. Estuarine variable (fDOM, NO3, Cl). Only rising limb data is shown here.

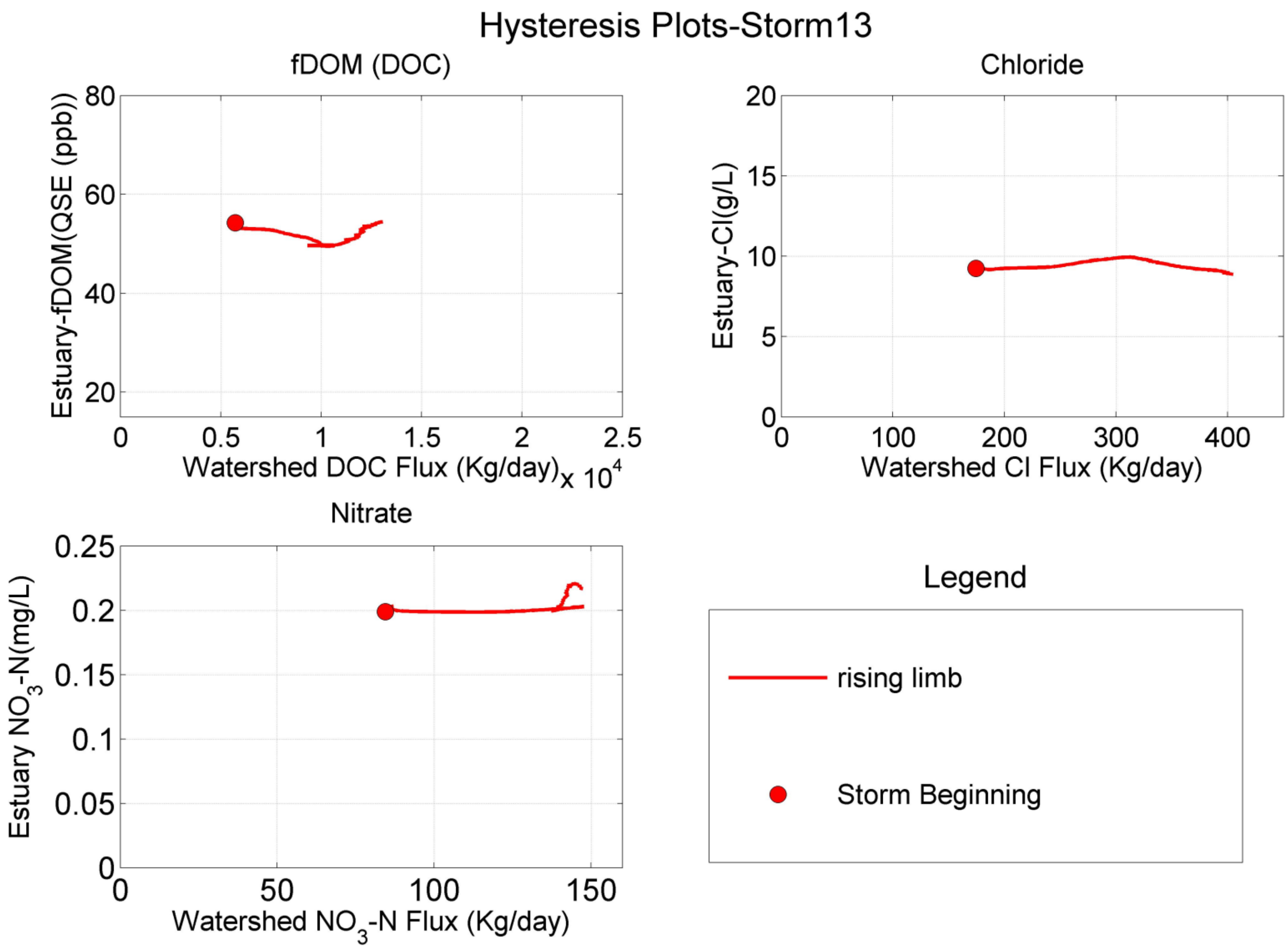

Figure S13 Hysteresis Pattern for one storm event, watershed variable (fluxes of DOC, NO_3 , and Cl) Vs. Estuarine variable (fDOM, NO3, Cl). Only rising limb data is shown here.

Aikman, F., & Lanerolle, L. W. J. (2005). *Report on the National Ocean Service Workshop on Residence / Flushing Times in Bays and Estuaries* (No. September). *NOAA*. NOAA Technical Report NOS CS 20.

Bilgili, A., Proehl, J. A., Lynch, D. R., Smith, K. W., & Swift, M. R. (2005). Estuary/ocean exchange and tidal mixing in a Gulf of Maine Estuary: A Lagrangian modeling study. *Estuarine, Coastal and Shelf Science*, *65*(4), 607–624. https://doi.org/10.1016/j.ecss.2005.06.027

Menke, W., & Menke, J. (2012). 9 - Detecting correlations among data. In W. Menke & J. Menke (Eds.), *Environmental Data Analysis with MatLab* (pp. 167–201). Boston: Elsevier. http://dx.doi.org/10.1016/B978-0-12-391886-4.00009-X